EFFECT OF ROTATION ON FLOW INSTABILITIES DURING SOLIDIFICATION OF A BINARY ALLOY

T.L. Sayre and D.N. Riahi
Departments of Theoretical and Applied Mechanics
(216 Talbot Laboratory, 104 S. Wright St.) and
Mechanical and Industrial Engineering (138 Mechanical
Eng. Building, 1206 W. Green St.)
University of Illinois,
Urbana, IL 61801

Abstract

Linear flow instabilities of the liquid and mushy regions during solidification of a binary alloy is investigated under a high gravity environment where the rotation axis is inclined to the high gravity vector. Results of stability analyses and numerical computations for a centrifugal mode of distrubance at several different rotation rates are determined which provide information for various flow features in the liquid and the mushy layers including neutral stability curves, streamlines and density plots for solid fraction perturbation in the mushy layer. The results indicate two distinct modes of convection whose dependences with respect to rotation rate suggest a procedure for possible elimination of chimneys formation tendency in the mushy layer. These chimneys are vertical channels of zero solid fraction and are kind of imperfections that reduce the quality of the solidified materials.

1. INTRODUCTION

The convection effects in directional solidification are known to be important [1]. The convective flow affects the solid-liquid content within the mushy layer adjacent to the solidified material and influences the flow pattern and the critical conditions for the onset of instabilities. It is important to reduce the undesirable effects of convection modes as much as possible for solidified system of the kind studied here and also find ways to prevent formation of localized chimneys within the mushy layer for such system, since it is known

that both effects of some convection modes and presence of chimneys can lead to defects and imperfections in the produced crystal. These chimneys are vertical channels of zero solid fraction that are also known as Freckles found in experiments dealing with solidified ingots [2,3]. Freckles are imperfections that reduce the quality of the solidified materials.

The rotational effects on the convective flow instabilities in the melt adjacent to the crystal interface have been of interest to the crystal growing community for many years. In industrial crystal growth processes it has been desirable to impose certain external constraint, such as rotation, in an optimized manner, upon the system in order to reduce the effects of such instabilities which can lead to microdefect density in the crystal and thus reduce the quality of the produced crystal. Theoretical normal gravity results on the effects rotation about a vertical axis on the melt during directional solidification of a binary alloy in the absence of a mushy layer [4,5] indicated conditions under which rotation can stabilize the convective flow. Computational results about the effects of steady vertical rotation on fluid motion during unidirectional solidification of a binary alloy [6] indicated stabilization of vertical plumes and their lack of meandering due to such rotational constraint. Sample and Hellawell [7,8] did NH_4Cl alloy experiment in a cylindrical mold with a chilled bottom surface where solidification was induced. They employed a rotation and tilting technique to change the orientation of gravity relative to the bottom surface of the cylinder. They found that for slow and steady rotation of the mold about the vertical axis, the channel formation and development was about the same as in the case without rotation. However, for slow and steady rotation of a tilted mold, the number of channels was reduced substantially and, under some conditions, completely eliminated. Fast rotation case is not considered beneficial to crystal growers as, for example, experimental results due to Rou et al. [9] indicated that if rotational speeds became too large, then segregates formed along a ring between the axis and outer edge of the ingot in his apparatus.

The experimental results discussed above indicate the possible usefulness of inclined rotational constraint applied on the solidified system. A solidified system under a high gravity environment provides a useful industrial example where an inclined rotation can operate effectively. The results of the two recent international workshops on Materials Processing in High Gravity (Dubna, Soviet Union, May 1991; Potsdam, USA, June 1993) indicated clear need for fundamental theoretical and computational understanding of the fluid dynamics of solidifying melts and, in particular, the effects of inclined rotation on the melt motion. A number of presented experimental results in these workshops as well as earlier reported experimental results in a centrifuge such as those due to Rodot et al. [10] indicated that at some high gravity levels undesirable convection effects can be suppressed and desirable high quality crystals can be grown. The present theoretical and computational studies consider linear instabilities of the liquid and mushy regions during solidification of a binary alloy and under the high gravity constraint in order to determine the effects of an inclined rotation at different gravity levels on the convection and the mushy layer structure and, in particular, on the chimneys formation tendency of the solidified system. An interesting result of the present investigation is that the spatial locations in the mushy layer that have tendency for chimney formation change as rotation rate increases or decreases. This result suggests an important operating procedure for possible elimination of chimneys formation tendency to be solidification under a variable rotational rate constraint in a high gravity environment.

2. MATHEMATICAL FORMULATION

We consider a thin layer of a binary alloy melt of some constant composition C_o and temperature T_∞ which is solidified at a constant rate V_o, with the eutectic temperature T_e at the position $z = o$ held fixed in a frame moving with the solidification speed in $z-$direction, where the $z-$axis is assumed to be anti-parallel with the high gravity vector to be described below (Figure 1). The physical model at normal gravity conditions is based on the assumptions of the type considered by Worster [11,12], and we refer the reader to

these references for details regarding such assumptions. The extension of such model in high gravity environment is done based on the assumptions of the type considered by Arnolds et al. [13] for solidification in a centrifuge, and we refer the reader to this reference for details regarding such high gravity considerations. Within the layer of melt, there is a very thin mushy layer adjacent to the solidifying surface and of thickness $h(x,y,t)$, where t is time variable and x and y axes are in a plane $(z=o)$ perpendicular to $z-$axis. We assume that the solidifying system is placed in a centrifuge basket rotating at some constant angular velocity Ω about the centrifuge axis which makes an angle γ with respect to $z-$axis. The centrifuge axis is anti-parallel to the earth gravity vector (Figure 2).

Next, we consider the equations for momentum, continuity, heat and solute for both liquid region $(z>h)$ and mushy region $(o<z<h)$ in the moving frame $oxyz$ whose origin o is centered on the solid-mush interface $(z=o)$, which is assumed to be flat [12]. The governing system of these equations for solidifying system rotating with the centrifuge basket [13] and translating with the solidification front at speed V_o is non-dimensionalized by using V_o, K/V_o, K/V_o^2, $\beta\Delta C\mathrm{P}_o g\, K/V_o$, ΔC and ΔT as scales for velocity, length, time, pressure, solute and temperature respectively. Here K is the thermal diffusivity, P_o is a reference (constant) density, $\beta=\beta*-T\alpha*$, where $\alpha*$ and $\beta*$ are the expansion coefficients for heat and solute respectively and T is the slope of the liquidus curve [11], which is assumed to be constant, $\Delta C\equiv C_o-C_e$, C_e is the eutectic concentration of the alloy, $\Delta T=T_L(C_o)-T_e$, and T_L is the local liquidus temperature. Due to the variations of density with respect to solute concentration and temperature, the centrifugal acceleration terms in the momentum equations for both liquid and mushy layers can not be converted into passive gradient terms and become important at significant rotation rate. Some recent results due to Riahi [5] indicate that there can be unusual and unexpected effects due to centrifugal acceleration term for a normal gravity soldifying system in the absence of mushy layer. The centrifugal acceleration term in the momentum equation, for either liquid or mushy layer, is then splitted into an average term, which is superimposed on the gravity

term, and a so-called gradient acceleration term [13]. The non-dimensional parameter representing the modified gravity term can then become significantly larger than the corresponding one due to earth's gravity alone for significant rotation rate. Following [11,12,14], we treat the mushy layer as a porous medium where Darcy's law is adopted.

The non-dimensional form of the governing equations and the boundary conditions for the liquid and mushy layers are given below based on the Worster [12] simplifying assumptions that $\beta = \beta *$, negligible temperature contribution to the buoyancy in the liquid zone and $K >> D$, where D is the solute diffusivity. The non-dimensional form of the equation for the momentum, continuity, temperature and solute concentration in the liquid layer $(z > h)$ are

$$\frac{1}{\mathrm{Pr}}\left(\frac{\partial}{\partial t} - \frac{\partial}{\partial z} + \underset{\sim}{u}\cdot\nabla\right)\underset{\sim}{u} = \nabla^2\underset{\sim}{u} - R_l\left(\nabla \mathrm{P} + S\hat{K}\right) - T_l\hat{\Omega}\times\underset{\sim}{u} - A_l S\underset{\sim}{R}, \tag{1a}$$

$$\nabla\cdot\underset{\sim}{u} = o, \tag{1b}$$

$$\left(\frac{\partial}{\partial t} - \frac{\partial}{\partial z} + \underset{\sim}{u}\cdot\nabla\right)\theta = \nabla^2\theta, \tag{1c}$$

$$\left(\frac{\partial}{\partial t} - \frac{\partial}{\partial z} + \underset{\sim}{u}\cdot\nabla\right)S = E\nabla^2 S, \tag{1d}$$

where $\underset{\sim}{u}$ is the velocity vector, P is the pressure, S is the solute concentration, θ is the temperature, $\hat{\Omega}$ is a unit vector along the rotation axis defined by

$$\hat{\Omega} = \cos\gamma\hat{K} + \sin\gamma\hat{i}, \tag{1e}$$

$\hat{K}$ is a unit vector along $z-$ axis, $\hat{i}$ is a unit vector along $x-$axis, $\underset{\sim}{R}$ is a radial position vector from the rotation axis defined by

$$\underset{\sim}{R} = \left(z\sin\gamma - x\cos\gamma\right)\left(\hat{i}\cos\gamma - \hat{K}\sin\gamma\right) - y\hat{j}, \tag{1f}$$

$\hat{j}$ is a unit vector along $y-$axis, $P_r = \mu/K$ is the Prandtl number, μ is the Kinematic viscosity, $R_l = \beta * \Delta C N_g K^2/(V_o^3 \mu)$ is the liquid solutal Rayleigh number, $T_l = 2\Omega K^2/(V_o^2 \mu)$ is the liquid Coriolis parameter (square root of Taylor number), $A_l = \beta \Delta C \Omega^2 K^3/(V_o^4 \mu)$ is the liquid gradient acceleration parameter, $N_g = (g^2 + \Omega^4 R_o^2)^{\frac{1}{2}}$ is the acceleration due to high gravity, $N = 1$ corresponds to normal gravity case while $N > 1$ indicates level of high gravity and $E = D/K$ (inverse of the Lewis number). The boundary conditions for the liquid layer are

$$\theta - S = \frac{\partial}{\partial z}(\theta - S) = \left[\hat{n} \cdot \underset{\sim}{u}\right] = \underset{\sim}{u} - \hat{n} \cdot \underset{\sim}{u} = o \text{ at } z = h, \tag{2a}$$

$$\theta \to \theta_\infty,\ S \to o,\ \underset{\sim}{u} \to o \text{ as } z \to \infty, \tag{2b}$$

where θ_∞ is the non-dimensional form of T_∞, the square brackets denote the jump in the enclosed quantity across the interface and $\hat{n}$ is a unit vector normal to the interface. The non-dimensional form of the equations for momentum, continuity, temperature and solute concentration in the mushy layer $(o < z < h)$ are

$$-\frac{\underset{\sim}{u}}{\Pi} = R_m\left(\nabla \mathrm{P} + S\hat{K}\right) + T_m \hat{\Omega} \times \underset{\sim}{u} + A_m S R, \tag{3a}$$

$$\nabla \cdot \underset{\sim}{u} = o, \tag{3b}$$

$$\left(\frac{\partial}{\partial t} - \frac{\partial}{\partial z} + \underset{\sim}{u} \cdot \nabla\right)\theta = \nabla^2 \theta + S_t\left(\frac{\partial}{\partial t} - \frac{\partial}{\partial z}\right)\phi, \tag{3c}$$

$$\left(\frac{\partial}{\partial z} - \frac{\partial}{\partial t}\right)\left[(1-\phi)(C_r - S)\right] + \underset{\sim}{u} \cdot \nabla S = E\nabla \cdot \left[(1-\phi)\nabla S\right], \tag{3d}$$

where $S_t = L/(C\Delta T)$ is the Stefan number, C is the specific heat per unit volume, L is the latent heat of solidification per unit volume, $C_r = (C_S - C_o)/\Delta C$ is a concentration ratio, C_s is the composition of the solid phase forming the dendrites, Π is the permeability of the mushy layer, ϕ is the local solid fraction of the mushy layer, $R_m = \beta \Delta C N_g \Pi_o/(V_o \mu)$ is the

mush solutal Rayleigh number, Π_o is a reference value of permeability, $T_m = 2\Omega\Pi_o/\mu$ is the mush Coriolis parameter and $A_m = \beta\Delta C\Pi_o K\Omega^2/(V_o^2\mu)$ is the mush gradient acceleration parameter. The boundary conditions for the mushy layer are

$$\theta = -1,\ \underset{\sim}{u}\cdot\hat{K} = o \text{ at } z = o \tag{4a}$$

$$[\theta] = [\hat{n}\cdot\nabla\theta] = [\mathrm{P}] = o \text{ at } z = h \tag{4b}$$

Analysis in Worster [12] indicates that $\theta = S$ in the mushy layer. This result is also valid here. For details regarding (1)-(4) and the assumptions involved the reader is referred to [11,12] on solidification aspects and to [13] on high gravity aspects.

Since we will consider two-dimensional solutions of (1)-(4) in (x,z) plane, it is convenient to eliminate the pressure terms in (1a) and (3a) by taking curl of these equations. We will seek solutions of the form

$$\begin{pmatrix}\theta\\ S\\ \underset{\sim}{u}\\ \phi\end{pmatrix} = \begin{pmatrix}\theta_o(z)\\ S_o(z)\\ o\\ \phi_o(z)\end{pmatrix} + \begin{pmatrix}\theta_1(z)\\ S_1(z)\\ u_1(z)\\ \phi_1(z)\end{pmatrix}\exp(B) + \begin{pmatrix}\theta_2(x,z)\\ S_2(x,z)\\ \underset{\sim 2}{u}(x,z)\\ \phi_2(x,z)\end{pmatrix} \tag{5a}$$

where $$B = i(wt + \alpha x), \tag{5b}$$

i is the pure imaginary number $(\sqrt{-1})$, w is the frequency of the perturbation, α is the wave number of the perturbation, quantitites with subscript `$o$´ denote base flow quantities [12], perturbation quantities with subscript `1´ and `2´ are small in comparison with the base flow quantities whose expressions are given below [12]

$$\theta_o(z) = \theta_\infty + (\theta_i - \theta_\infty)\exp(h_o - z), \qquad (z > h_o), \tag{6a}$$

$$S_o(z) = \theta_i \exp[(h_o - z)/E], \qquad (z > h_o), \tag{6b}$$

$$z=\left(\frac{\alpha_1-C_r}{\alpha_1-\beta_1}\right)ln\left(\frac{\alpha_1+1}{\alpha_1-\theta_o}\right)+\left(\frac{C_r-\beta_1}{\alpha_1-\beta_1}\right)ln\left(\frac{\beta_1+1}{\beta_1-\theta_o}\right), \qquad (o<z<h_o), \quad (6c)$$

$$S_o(z)=\theta_o(z), \qquad (o<z<h_o), \quad (6d)$$

where

$$\alpha_1=A_1+B_1,\ \beta_1=A_1-B_1,\ A_1=\left(C_r+\theta_\infty+S_t\right)/2,\ B_1^2=A_1^2-C_r\theta_\infty-S_t\theta_i, \quad (6e)$$

h_o is the mush-liquid interface at the fixed (constant) z level, θ_i is the interfacial temperature given by

$$\theta_i=E\theta_\infty/(E-1), \quad (6f)$$

and it should be noted that the expression for θ_o in the mushy layer is given implicitly in terms of z.

Next, (5a) is used in the governing system, multiply each equation and boundary condition by $\exp(-B)$, linearize the system with respect to the amplitude of the perturbations, and then take the average of the resulting system with respect to the x variable. We shall investigate numerically the following resulting system of equations and the boundary conditions in the limit of zero value of the quantities with subscript `2´. In the liquid region $(z>h)$, the equations are

(7a)

$$\left[D_3^2+\left(D_3-iw\right)/\mathrm{P}_r-\alpha^2\right]\Omega_1+\alpha^2R_tS_1+i\alpha A_t\sin\gamma\left(z\cos\gamma D_3+\cos\gamma+i\alpha z\sin\gamma\right)S_1=o,$$

$$\left(ED_3^2+D_3-iw-E\alpha^2\right)S_1=W_1D_3S_o, \quad (7b)$$

$$\left(D_3^2-\alpha^2\right)W_1=\Omega_1, \quad (7c)$$

$$\left(D_3^2+D_3-iw-\alpha^2\right)\theta_1=W_1D_3\theta_o, \quad (7d)$$

where $D_3\equiv\dfrac{\partial}{\partial z}$ and Ω_1 represents the perturbation vorticity.

These equations are subjected to the following boundary conditions:

$$\theta_1 - S_1 = [W_1] = D_3 W_1 = D_3(S_1 - \theta_1) + (E-1)\eta_1 D_3\theta_o / E = o \text{ at } z = h_o, \quad (8a)$$

$$\theta_1 \to o,\ S_1 \to o,\ W_1 \to o,\ D_3 W_1 \to o \text{ as } z \to \infty, \quad (8b)$$

where $\eta_1(x,t) = (h - h_o)\exp(-B)$.

In the mushy region $(o < z < h)$, the equations are

$$\left\{D_3^2 + \left[1 + S_t(C_r - \theta_i)/(C_r - \theta_o)^2\right](D_3 - iw) + 2S_t(C_r - \theta_i)D_3\theta_o/(C_r - \theta_o)^3 - \alpha^2\right\}$$
$$\theta = S_t\xi_1 D_3\theta_o/(C_r - \theta_o)^2 + \left[1 + S_t/(C_r - \theta_o)\right]WD_3\theta_o, \quad (9a)$$

$$\left\{D_3^2 - \left(\Pi'(xo)(C_r - \theta_i)D_3\theta_o/\left[\Pi(x_o)(C_r - \theta_o)^2\right]\right)D_3 - \alpha^2\right\}$$
$$W_1 = \alpha^2\Pi_o R_m\theta_1 + i\alpha\Pi_o \sin\gamma A_m(\cos\gamma z D_3 + \cos\gamma + i\alpha\sin\gamma z)\theta_1, \quad (9b)$$

$$(D_3 - iw)\xi_1 = WD_3\theta_o, \quad (9c)$$

where $\xi_1 \equiv xS_1 + \phi_1 C_r$, $x = 1 - \phi$ is the liquid fraction, $x_o = (C_r - \theta_i)/(C_r - \theta_o)$ is the unperturbed porosity, Π' denotes derivative of Π with respect to x and Π_o is a constant reference value for Π which will be set equal to one later in the numerical procedure.

The equations in the mushy layer are subjected to the following boundary conditions:

$$[\theta_1] = [D_3\theta_1] + S_t\eta_1 D_3\theta_o/(C_r - \theta_i) = \xi_1 - \theta_1 - \eta_1 D_3\theta_o = 0 \text{ at } z = h_o, \quad (10a)$$

$$R_l D_3 W_1|_{mush} = -R_m\Pi(1)\left[D_3\Omega_1 + (\Omega_1 + \alpha^2 W_1)/P_r\right]_{liquid} \text{ at } z = h_o, \quad (10b)$$

$$\theta_1 = W_1 = o \text{ at } z = o \quad (10c)$$

3. NUMERICAL PROCEDURE

In this paper we consider only the onset of stationary $(w = o)$ two-dimensional linear instabilities [12]. Due to complexity of the system (7)-(10), persisted even with such consideration, we use a numerical procedure of the type developed and utilized by Worster

[12]. Here we describe this numerical approach briefly and refer the reader to [12] for details of the procedure. Define

$$\tau = \theta_\infty - \theta_o \qquad (o \le \tau \le \tau_e) \tag{11}$$

as the new independent variable, where $\tau_e \equiv 1 + \theta_\infty$, and $\tau = o$ and τ_e correspond, respectively, to $z = \infty$ and o. This approach has the additional advantage that the transcendental equation (6c) is not needed to be inverted. Using (11) in (7)-(10), leads to a system of ordinary differential equations for W_1, Ω_1, θ_1, S_1, and ξ_1 as functions of independent variable τ. Due to two-dimensional character of the disturbances, Coriolis effects do not enter the analysis and following [12] we find that the following relation holds

$$R_l / R_m = A_l / A_m = H, \tag{12}$$

where H is generally a large parameter [12]. The new form of the governing stability system has a regular singular point at $\tau = o$ [12]. Following Worster [12], we write

$$(\theta_1, S_1, W_1, \Omega_1) = \tau^m \left(\tilde{\theta}, \tilde{S}, \tilde{W}, \tilde{\Omega}\right), \qquad o < \tau < \tau_i, \tag{13}$$

in the liquid region, where $\tau_i \equiv \theta_\infty / (1 - E)$ corresponds to value of $z = h_o$ at the mush-liquid interface and m is a root of the indicial equation. We then use the numerical procedure to solve for the analytic functions $\left(\tilde{\theta}, \tilde{S}, \tilde{W}, \tilde{\Omega}\right)$. Using (13) in the governing equations in the liquid region lead to four linearly independent solutions that satisfy the boundary conditions at $\tau = o$ corresponding to four values of m given by

$$m_1 = \left[1 + \left(1 + 4\alpha^2\right)^{\frac{1}{2}}\right] \Big/ 2, \quad m_2 = \left[E^{-1} + \left(E^{-2} + 4\alpha^2\right)^{\frac{1}{2}}\right] \Big/ 2,$$
$$m_3 = \left[\mathrm{P}_r^{-1} + \left(\mathrm{P}_r^{-2} + 4\alpha^2\right)^{\frac{1}{2}}\right] \Big/ 2, \quad m_4 = \alpha \cdot \tag{14}$$

When $m = m_i$, the corresponding values of $\left(\tilde{\theta}, \tilde{S}, \tilde{\Omega}, \tilde{W}\right)$ at $\pi = o$ are found from (18b) and the governing equations for these variables and are given below by the $i-th$ row of

i	$\tilde{\theta}$	$\tilde{S}$	$\tilde{\Omega}$	$\tilde{W}$
1	1	o	o	$\tilde{\Omega}/\left(m^2-\alpha^2\right)$
2	o	1	$\tilde{\Omega}_2/\left(m^2-P_r^{-1}m-\alpha^2\right)$	$\tilde{\Omega}/\left(m^2-\alpha^2\right)$
3	o	o	1	$1/\left(m^2-\alpha^2\right)$
4	o	o	o	1

where

$$\tilde{\Omega}_2 = -\alpha^2 R_l + i\alpha A_l \sin\gamma\left\{\left[h_o + 1n\left(\tau_i/\tau_s\right)\right]\left(\cos\gamma m_2 - i\alpha\sin\gamma\right) - \cos\gamma\right\}$$

Also, for each value of $m = m_i$, a Taylor series expansion of the governing equations for $\left(\tilde{\theta}, \tilde{S}, \tilde{\Omega}, \tilde{W}\right)$ about $\tau = o$ was applied to determine the first three derivatives of the dependent variables at $\tau = o\cdot$. These results allow numerical evaluation of the governing equations for $\left(\tilde{\theta}, \tilde{S}, \tilde{\Omega}, \tilde{W}\right)$ in the liquid region to be started from the asymptotic expressions for the dependent variables near $\tau = o$. We applied an efficient Runge-Kutta scheme of fourth order for this purpose. For each value of m, the governing equations are integrated from $\tau = o$ to $\tau = \tau_i$. Next, we used (8a) and (10a,b) to relate the dependent variables in the mushy layer at $\tau = \tau_i$ to the dependent variables in the liquid region. These values are used to start the numberical integration of the governing equations for $\left(\theta_1, \xi_1, W_1\right)$ in the mushy region at $\tau = \tau_i$, which continues until $\tau = \tau_e$. Note that $S_1 = \theta_1$ in the mushy region [12] and there is no need for separate equation for Ω_1 since Ω_1 is given in terms of W_1 and $D_3^2 W_1$ like (7c). However, the resulting solution will not, in general, satisfy all the boundary conditions. The remaining boundary conditions are used to compute the following residuals r_{ij} corresponding to index m_i :

$$r_{i1} = \tau^{mi}\left(\tilde{\theta} - \tilde{S}\right) \text{ at } \tau = \tau_i$$

$$r_{i2} = \tau^{mi}\frac{\partial \tilde{W}}{\partial \tau} + m_i \tau^{mi-1}\tilde{W} \text{ at } \tau = \tau_i$$

$$r_{i3} = \theta_1 \text{ at } \tau = \tau_e$$

$$r_{i4} = W_1 \text{ at } \tau = \tau_e$$

The determinant of the matrix $\left[r_{ij}\right]$,

$$Det = Det\left(R_m, \alpha; E, H, P_r, S_t, C_r, \theta_\infty A_m\right),$$

is then computed, and R_m is varied until $Det = o$. The corresponding solutions are eigen functions of the governing stability system which represent the marginally stable stationary states of the system.

4. RESULTS

Following [12], we set $\gamma = 30^\circ, S_t = C_r = \theta_\infty = 1$, $P_r = 10$ unless otherwise stated and $\Pi(x) \equiv 1$. The eigen value relation $Det = o$ then will provide a marginal stability curve $R_m(\alpha)$ for each choice of the parameters E, H and A_m. The parameter E is the inverse of Lewis number and is typically very small. The parameter H is a representative of the square of the ratio of the thermal length scale, on which the depth h depends, to the average spacing between dendrites within the mushy layer [12]. This parameter is typically very large. The gradient acceleration parameter A_m will be assigned the values 0, 0.1, 0.3 and 0.6 which turns out to represent adequately the several degrees of rotational strengths in the present model. The values chosen for E and H are similar to those chosen by Worster [12].

The results for neutral stability curve, R_m versus α for several values of A_m and for values of $E = 0.025$ and $H = 10^5$ are shown in figure 3. The system is unstable in the region above each of the curve and is stable below the curve. Just as in the zero rotation case $\left(A_m = 0\right)$, the marginal curve for each value of A_m has two minima, corresponding to two distinct modes of convection. The first mode, corresponding to the first minimum with smaller α, is called here long wavelength mode since its wavelength is comparable to

h and causes flow throughout the mushy layer, while the second mode, corresponding to the second minimum with larger α, is called short wavelength mode since its wavelength is comparable to the depth of the compositional boundary layer ahead of the mush-liquid interface and leaves the fluid within the interstices of the mushy layer essentially stagnant [12]. These properties can be confirmed by observation of the streamlines plots to be discussed below. It is seen from the results presented in figure 3 that R_m increases with A_m for a given α and the wave numbers of the two modes increase with A_m. Hence, rotation has the familiar effects of increasing the critical values of A_m and α [15].

Streamlines for the two convection modes corresponding to the local minima of the neutral stability curves of figure 3 are presented in figures 4-11 for several different values of A_m. It is seen from these figures that, for zero rotation $(A_m = 0)$ case, fluid flows deeply in the liquid and mushy zones for the long wavelength mode (figure 4), while flow is retricted to a thin region about the mush-liquid interface for the short wavelength mode (figure 5). For non-zero rotation cases, fluid flows in both liquid and mushy regions and is stronger in the later regions for the long wavelength mode. As rotation increases, flow is stabilized more strongly in the liquid layer (figure 6, 8 and 10). For the short wavelength mode, the flow is restricted to the mushy layer only, but such flow is more close to the mush-solid interface for larger rotation rate (figures 7, 9 and 11).

Tables 1-8 provide information about the vertical velocity and horizontal velocity designated there, respectively, by $w(x,z)$ and u(x,z) in both liquid and mushy regions and for both of the convection modes. It is seen that the magnitude of velocity in the liquid region is generally larger than the corresponding one in the mushy region, while the opposite is generally true for non-zero rotation cases. Also for each case the magnitude of the velocity for the long wavelength mode is generally larger than the corresponding one for the short wavelength mode.

Density plots of the perturbation to the solid fraction in the mushy region for both convective modes and for different values of A_m are shown in figures 12-19. Dark and light regions correspond respectively, to local melting and enhanced solidification regions. It is seen from these figures that the short wavelength mode causes less perturbation to the solid fraction than the long wavelength mode. The long wavelength mode is, thus, mostly associated with the solid fraction perturbations. For this mode, there is a substantial decrease in the solid fraction in the interior of the mushy layer in regions of up flow which indicates a tendency to form chimneys. The information provided by these figures for different values of A_m indicate that the spatial locations in the mushy region which have tendency to form chimneys, that is dark regions in the figures corresponding to negative perturbation to the solid fraction that represent local melting of the dendrites, change as rotation rate increases or decreases. This interesting result suggests an important operational procedure for possible elimination of chimneys formation tendency to be a variable rotational rate constraint applied on the solidifying system.

The results shown in the figure 3 for the dependence of the neutral stability curve on A_m are for fixed values of $E = 0.025$ and $H = 10^5$. It turns out that the relative stability of the two convection modes varies considerably with the values of H and E. A particular interpretation of H is as a measure of the relative mobility of fluid in the melt region to that in the mushy layer [12]. Thus, increasing H causes the melt region to become more unstable relative to the mushy layer. The results from the marginal stability curves for various values of H with $E = 0.025$ held fixed shown in figures 20-23 confirm such interpretation of the parameter H. These figures also show that either of the two convection modes can be the most unstable one depending on the parameters of the system. In particular, the short wavelength mode is the most unstable one for $A_m = 0.3$ and $H = 2(10)^5$ (figure 23a), while the long wavelength mode is the most critical one for $A_m = 0.1$ and $H = 6.4\left(10^4\right)$ (figure 22b). It seems that the long wavelength mode is the most unstable one for sufficiently strong rotation (figure 23b) or for sufficiently small

H (figure 20) while the short wavelength mode is the most unstable one for weak rotation provided H is sufficiently large (figures 22 and 23a).

In regard to variation of E, it should be stated that the main effect of such variation is to change the thickness of the compositional boundary layer ahead of the mush-liquid interface relative to the depth of the mushy layer, and the thickness of the compositional boundary layer decreases with decreasing E [12]. Marginal stability curves for various values of E and A_m with $H = 10^5$ are shown in figures 24-26. It is seen from these figures that the convection modes become more stabilized as E decreases, and this is more strongly true for the boundary layer mode. The wavelength of the short wavelength mode decreases with decreasing E. Destabilizing effect of relatively larger E on the short wavelength mode is seen in figure 26c. Rotational effects seem to be minimized for some intermediate value of E (figure 26b).

The results discussed so far were for the cases of aqueous solutions where $P_r = 10$ is representative. However, metallic alloys, which are of commercial interest, have representative value of 0.02 for P_r. Therefore, it is of interest to compare some results for these two different P_r values cases. Marginal stability curves for these two different values of P_r with $E = 0.01$, $H = 10^6$ and various values of A_m are shown in figures 27-29. It is seen from these figures that the system is more stable at lower P_r and that the wavelength of the long wavelength mode for the lower P_r is smaller than the corresponding one for the higher P_r. As discussed by Worster [12], the inverse Prandtl number P_r^{-1} measures the strength of the advection or diffusion of vorticity generated by buoyancy, due to the solidification growth rate velocity V_o, and, thus, the smaller P_r, the larger is the advection of such vorticity towards the solid boundary, which acts as a sink of vorticity due to no-slip condition. Thus system tends to be more stable for smaller P_r.

5. DISCUSSION

The results of the present study indicates that rotational effects due to gradient acceleration terms in the momentum equations can significantly affect the flow structure in

both liquid and mushy layers. Our stability analysis detected two distinct modes of convection. The two modes which have been found earlier by Worster [12] in the case without rotation, agree with our case $A_m = o$. Worster called one boundary layer mode since it was associated with the compositional buoyancy in a thin boundary layer just above the mush-liquid interface and had a critical wavelength comparable to the thickness of such boundary layer. He called the second one mushy layer mode since it was driven by the buoyancy in the interior of the mushy layer and had a wavelength comparable to the depth of the mushy layer. In the present study for non-zero A_m, we find that such a characterization of these modes is no-longer appropriate since rotational effects alter significantly the form of these modes. For example, figures 7, 9 and 11 show that the mode, referred to as boundary layer mode in [12], occupies most of the mushy layer and leave liquid layer virtually stagnant. Also figures 6, 8 and 10 show that the mode, referred to as mushy layer mode in [12], is much stronger in the system than the corresponding one for $A_m = 0$ (figure 4). Hence, we decided to call these two modes as short wavelength and long wavelength modes since they have distinct short and long wave length characteristics which persist even in the case of strong rotation. We found that rotational effects make both of these modes more dependent on the internal structure of the mushy layer and results in negative perturbations of the solid fraction that are indicative of the chimneys formation tendencies, although the long wavelength mode seems to be more effective in this negative solid fraction perturbations process. An interesting result of the present rotational studies is that the spatial locations in the mushy layer which have tendency to form chimneys change as rotation rate changes. The result suggests an important industrial operational procedure for possible elimination of Freckles formation tendency to be a variable rotational rate constraint applied on the solidifying system..

It is of interest to note from the stability system (7)-(10) that rotational effects disappear for $\gamma = 0$. That is, rotational constraint is effective here only if the rotation axis is inclined to the $z-$axis which is anti-parallel to the high gravity vector. This result

indicates the significance of the high gravity environment which provides an effective rotational constraint.

As is indicated from the results presented in the previous section, the present two-dimensional stability analysis does not include the effects of the Coriolis force terms in the momentum equations. Such effects can be included in a three-dimensional stability analysis which is hoped to be accomplished by the second author in the near future. Some preliminary investigation by the present authors on the three-dimensional stability analysis of the problem indicates that such three-dimensional model modifies significantly the present numerical code and, in particular, the parameter m now has 5 values and consequently the matrix $\left[r_{ij}\right]$ has now a 5×5 determinant.

REFERENCES

[1] S.H. DAVIS, *J. Fluid Mech.* **212**, 241-262 (1990).

[2] S.M. COPLEY, A.F. GIAMEI, S.M. JOHNSON and M.F. HORNBECKER, *IMA J. Appl. Maths.,* **35**, 159-174 (1970).

[3] J.R. SARAZIN and A. HELLAWELL, *Metall. Trans.*, **19A**, 1861-1871 (1988).

[4] D.N. RIAHI, *Acta Mechanica*, **99**, 95-101 (1993).

[5] D.N. RIAHI, Materials processing in high gravity, edited L.L. Regel and W.R. Wilcox, (Plenum press, New York), 133-137 (1994).

[6] D.G. NEILSON and F.P. INCROPERA, *Int. J. Heat Mass Transfer*, **36**, 489-505 (1993).

[7] A.K. SAMPLE and A. HELLAWELL, *Met. Trans. B.*, **13B**, 495-501 (1982).

[8] A.K. SAMPLE and A. HELLAWELL, *Met. Trans. A.*, **15**, 2163-2173 (1984).

[9] S. KOU, D.R. POIRIER and M.C. FLEMINGS, *Metall. Trans. B.*, **9B**, 711-719 (1978).

[10] H. RODOT, L.L. REGAL and TURTCHANINOV, *J. Crystal Growth*, **104**, 280-284 (1990).

[11] M.G. WORSTER, *J. Fluid Mech.*, **224**, 335-359 (1991).

[12] M.G. WORSTER, *J. Fluid Mech.*, **237**, 649-669 (1992).

[13] W.A. ARNOLDS, W.R. WILCOX and F. CARLSON, *J. Crystal Growth*, **119**, 24-40 (1992).

[14] P.H. ROBERTS and D.E. LOPER, In stellar and Planetary Magnetism, edited A.M. Soward (Gorden and Breach), 329-349 (1983).

[15] S. CHANDRASEKHAR, Hydrodynamic and hydromagnetic stability, Oxford University Press (1961).

FIGURE CAPTIONS

Figure 1. A diagram representing the steady directional solidifciation of an alloy at speed V_o. A mushy layer between or solid region, where $T < T_e$, and a liquid region. The profiles for dimensional temperture and the local liquidus temperature T_L are also shown. L, η and S denote, respectively, liquid, mush and solid regions.

Figure 2. Solidification system in a centrifuge. C denotes the center of gravity of the centrifuge basket.

Figure 3. Marginal stability curves with $E = 0.025$, $H = 10^5$ and for $A_m = 0.,\ 0.1,\ 0.3,\ 0.6$.

Figure 4. Streamlines for the long wavelength $(A_m = 0,\ \alpha = 2.19,\ R_m = 7.64)$.

Figure 5. Streamlines for the short wavelength $(A_m = 0,\ \alpha = 12.93,\ R_m = 8.04)$.

Figure 6. Streamlines for the long wavelength $(A_m = 0.1,\ \alpha = 2.20,\ R_m = 7.71)$.

Figure 7. Streamlines for the short wavelength $(A_m = 0.1,\ \alpha = 12.95,\ R_m = 8.04)$.

Figure 8. Streamlines for the long wavelength $(A_m = 0.3,\ \alpha = 2.21,\ R_m = 8.15)$.

Figure 9. Streamlines for the short wavelength $(A_m = 0.3,\ \alpha = 13.55,\ R_m = 8.62)$.

Figure 10. Streamlines for the long wavelength $(A_m = 0.6,\ \alpha = 2.26,\ R_m = 9.40)$.

Figure 11. Streamlines for the short wavelength $(A_m = 0.6,\ \alpha = 15.40,\ R_m 10.25)$.

Figure 12. Density plot of the perturbation to the solid fraction in the mushy region for the long wavelength mode for $A_m = 0 \cdot$

Figure 13. Density plot of the perturbation to the solid fraction in the mushy region for the short wavelength mode for $A_m = 0 \cdot$

Figure 14. The same as in figure 12 but for $A_m = 0.1 \cdot$

Figure 15. The same as in figure 13 but for $A_m = 0.1 \cdot$

Figure 16. The same as in figure 12 but for $A_m = 0.3 \cdot$

Figure 17. The same as in figure 13 but for $A_m = 0.3 \cdot$

Figure 18. The same as in figure 12 but for $A_m = 0.6 \cdot$

Figure 19. The same as in figure 13 but for $A_m = 0.6 \cdot$

Figure 20. Marginal stability curves for $E = 0.025$ and various values of $\mathrm{A_m} \cdot$
a)$\mathrm{H} = 6.4(10)^4 \cdot$ b)$\mathrm{H} = 2(10)^4 \cdot$

Figure 21. Marginal stability curves for $E = 0.025$ and various values of $A_m \cdot$
$a) H = 10^5 \cdot \quad b) H = 2\left(10^5\right) \cdot$

Figure 22. Marginal stability curves for $E = 0.025$ and various values of $H \cdot$
$a) A_m = 0 \cdot \quad b) A_m = 0.1 \cdot$

Figure 23. Marginal stability curves for $E = 0.025$ and various values of $H \cdot$
$a) A_m = 0.3 \cdot \quad b) A_m = 0.6 \cdot$

Figure 24. Marginal stability curves for $H = 10^5$ and several values of $E \cdot$
$a) A_m = 0 \cdot \quad b) A_m = 0.1 \cdot$

Figure 25. Marginal stability curves for $H = 10^5$ and several values of $E \cdot$
$a) A_m = 0.3 \cdot \quad b) A_m = 0.6 \cdot$

Figure 26. Marginal stability curves for $H = 10^5$ and several values of $A_m \cdot$
$a) E = 0.0125 \cdot \quad b) E = 0.0175 \cdot \quad c) E = 0.025 \cdot$

Figure 27. Marginal stability curves for $E = 0.01$, $H = 10^6$ and $\mathrm{P}_r = 0.02,\ 10 \cdot$
$a) A_m = 0 \cdot \quad b) A_m = 0.1 \cdot$

Figure 28. Marginal stability curves for $E = 0.01$, $\mathrm{H} = 10^6$ and $P_r = 0.02,\ 10 \cdot$
$a) A_m = 0.3 \cdot \quad b) A_m = 0.6 \cdot$

Figure 29. Marginal stability curves for $E = 0.01$, $H = 10^6$ and various values of $A_m \cdot$
$a) P_r = 10 \cdot \quad b) P_r = 0.02 \cdot$

TABLE CAPTIONS

Table 1. Values of vertical velocity and horizontal velocity for both liquid and mushy zones for $A_m = 0,\ \alpha = 2.19,\ R_m = 7.64 \cdot$

Table 2. The same as in table 1 but for $A_m = 0,\ \alpha = 12.93,\ R_m = 8.04 \cdot$

Table 3. The same as in table 1 but for $A_m = 0.1,\ \alpha = 2.20,\ R_m = 7.71 \cdot$

Table 4. The same as in table 1 but for $A_m = 0.1,\ \alpha = 12.95,\ R_m = 8.04 \cdot$

Table 5. The same as in table 1 but for $A_m = 0.3,\ \alpha = 2.21,\ R_m = 8.15 \cdot$

Table 6. The same as in table 1 but for $A_m = 0.3,\ \alpha = 13.55,\ R_m = 8.62 \cdot$

Table 7. The same as in table 1 but for $A_m = 0.6,\ \alpha = 2.26,\ R_m = 9.40 \cdot$

Table 8. The same as in table 1 but for $A_m = 0.6,\ \alpha = 15.40,\ R_m = 10.25 \cdot$

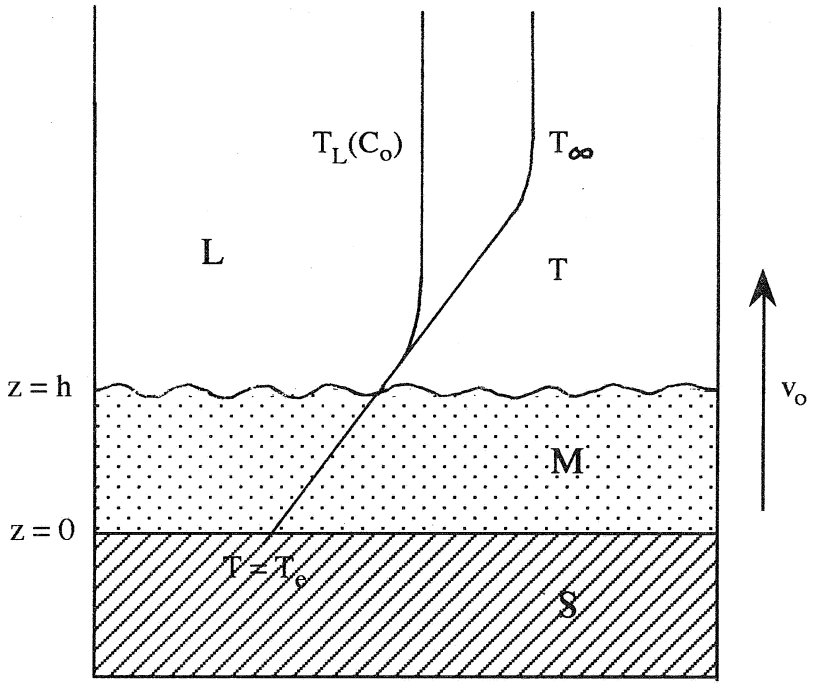

Figure 1

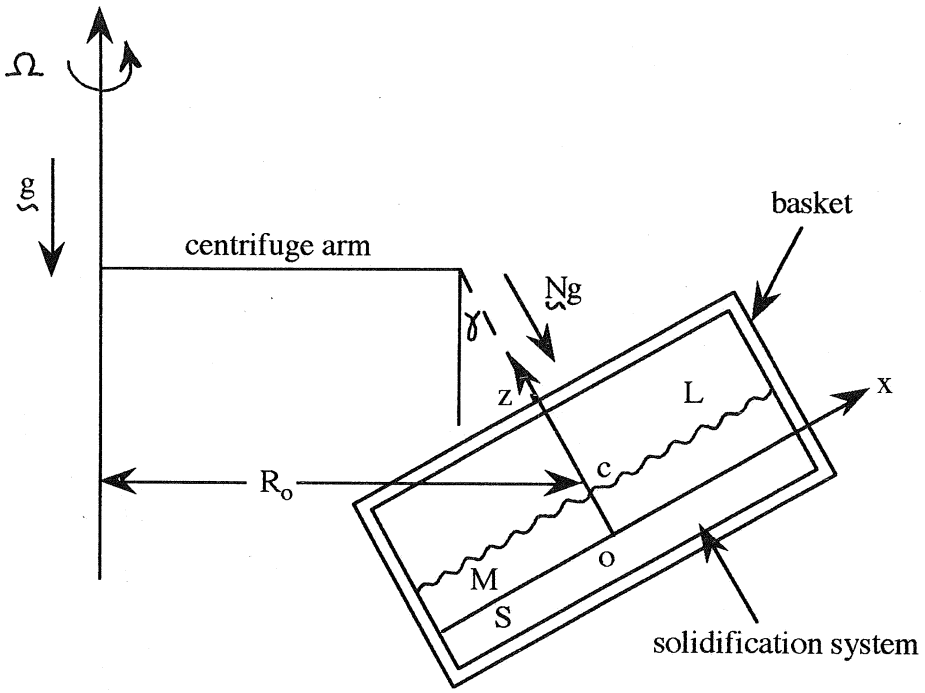
Ω
g
centrifuge arm
Ng
γ
basket
z
L
x
R_o
c
o
M
S
solidification system

Figure 2

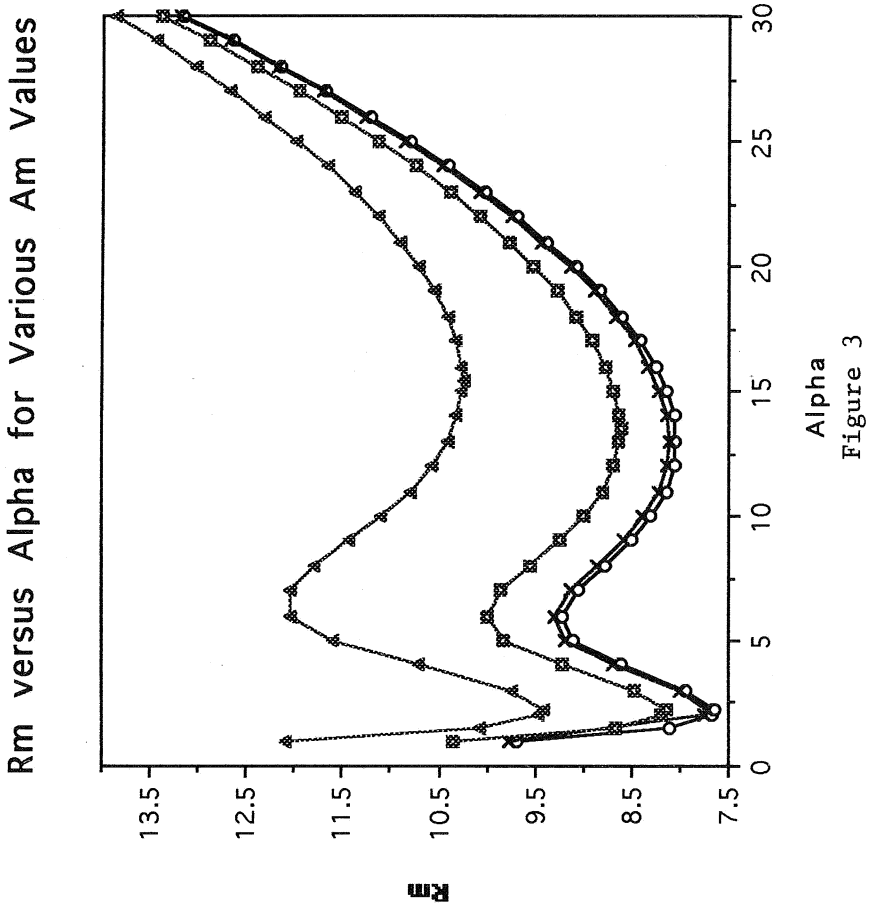
Rm versus Alpha for Various Am Values
Am=0
Am=0.1
Am=0.3
Am=0.6
Note: Al = (1E5)Am
Rm
13.5
12.5
11.5
10.5
9.5
8.5
7.5
0
5
10
15
20
25
30
Alpha

Figure 3

Stream Function for Am=0, Alpha=2.19, Rm=7.64

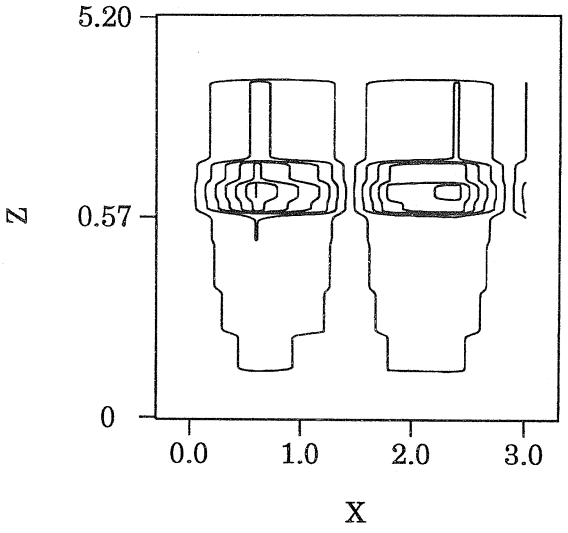

Figure 4

Stream Function for Am=0, Alpha=12.93, Rm=8.04

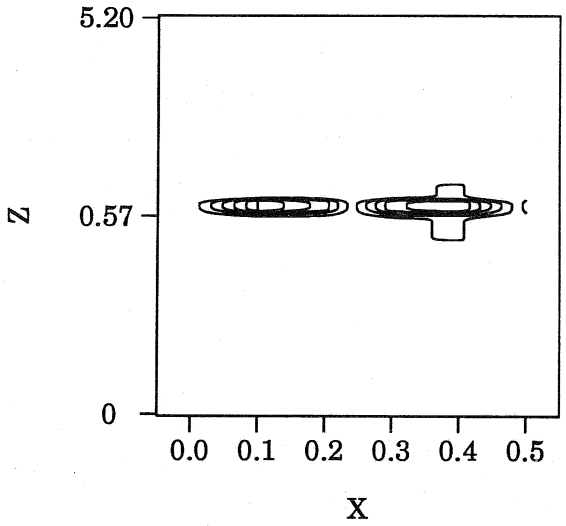

Figure 5

Stream Function for Am=0.1, Alpha=2.20, Rm=7.71

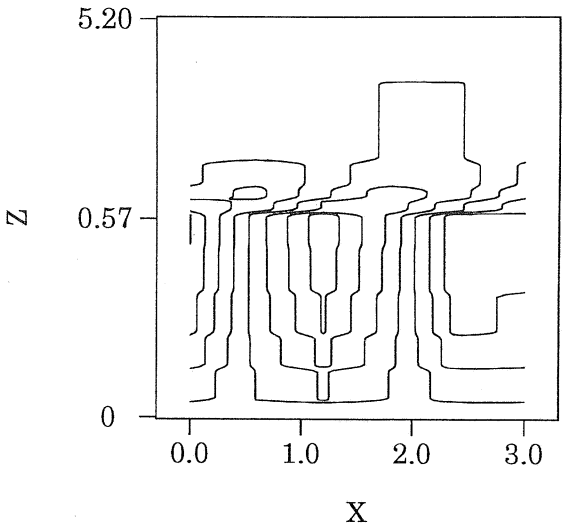

Figure 6

Stream Function for Am=0.1, Alpha=12.95, Rm=8.04

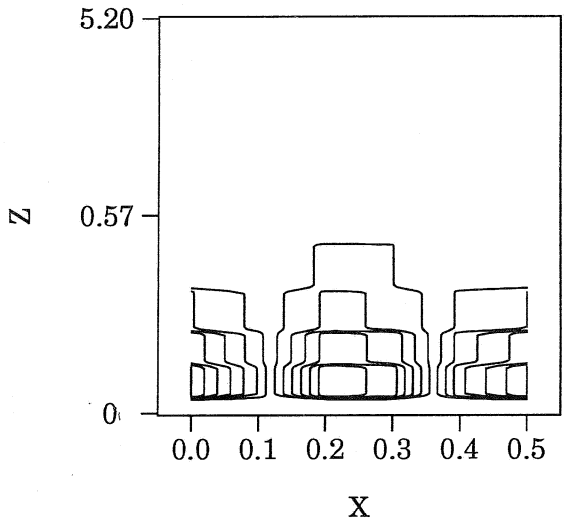

Figure 7

Stream Function for Am=0.3, Alpha=2.21, Rm=8.15

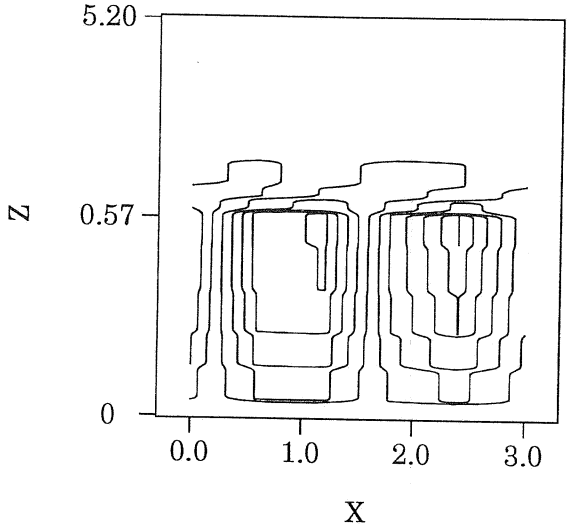

Figure 8

Stream Function for Am=0.3, Alpha=13.55, Rm=8.62

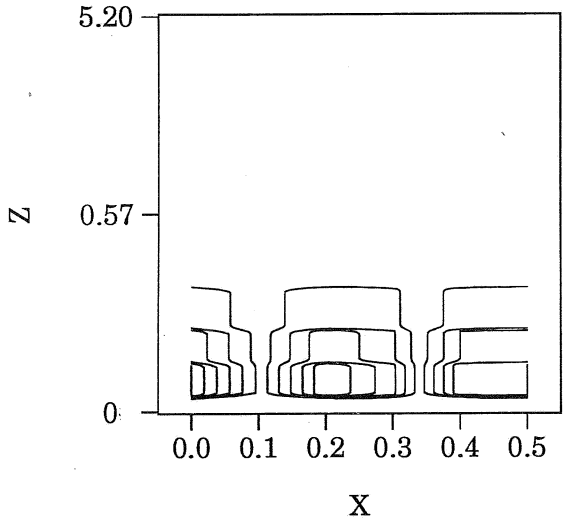

Figure 9

Stream Function for Am=0.6, Alpha=2.26, Rm=9.40

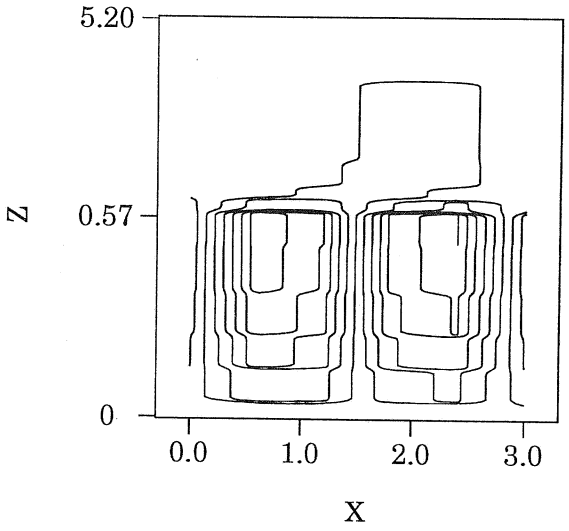

Figure 10

Stream Function for Am=0.6, Alpha=15.40, Rm=10.25

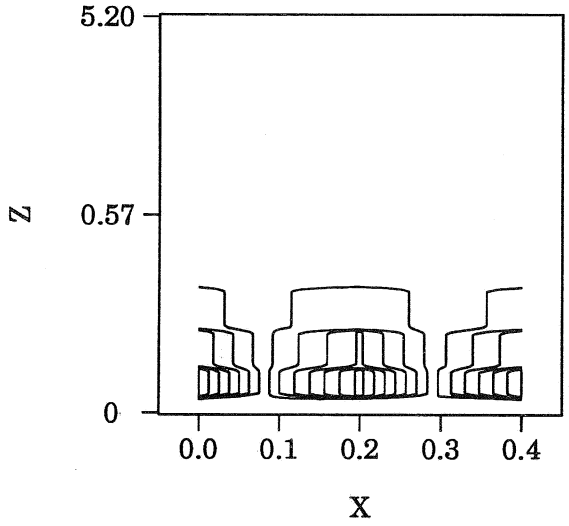

Figure 11

Perturbation of Solid Fraction for Am=0, Alpha=2.19, Rm=7.64

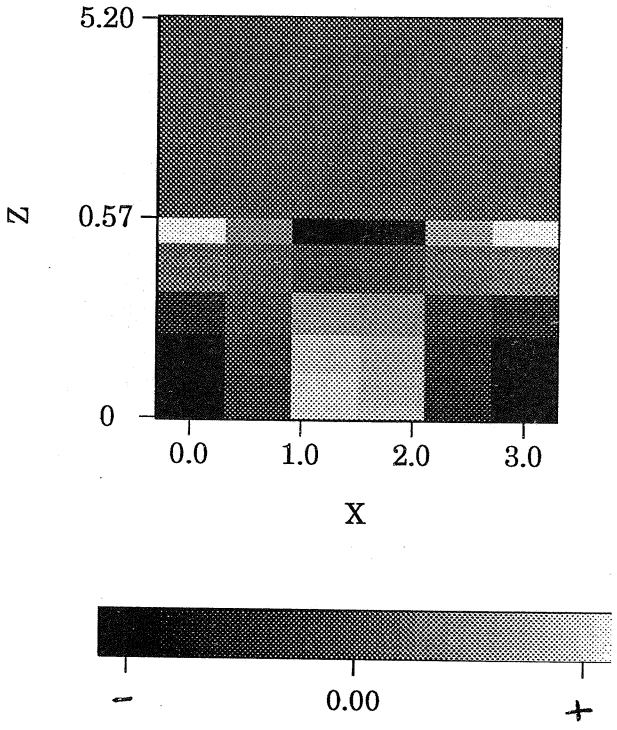

Figure 12

Perturbation of Solid Fraction for Am=0, Alpha=12.93, Rm=8.04

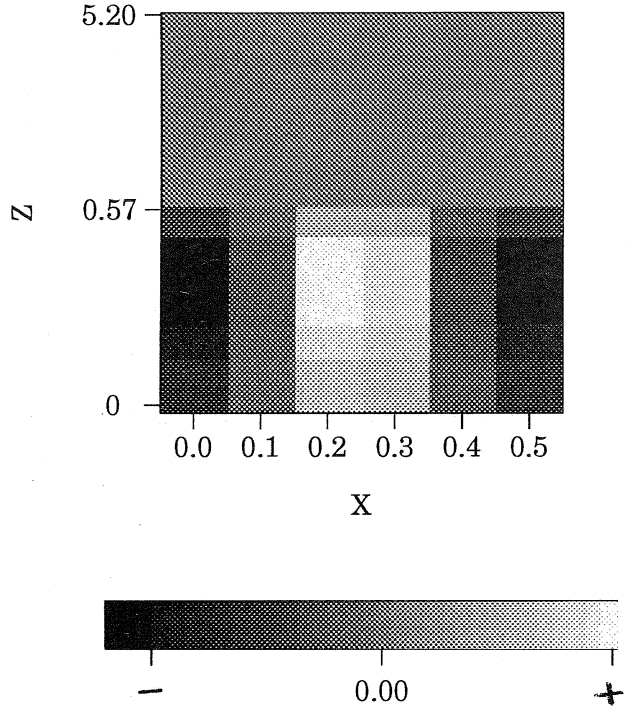

Figure 13

Perturbation of Solid Fraction for Am=0.1, Alpha=2.20, Rm=7.71

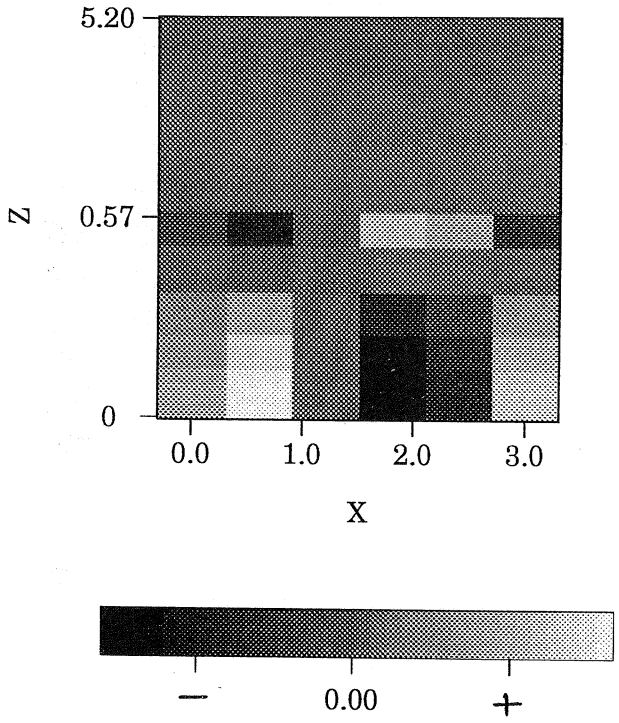

Figure 14

Perturbation of Solid Fraction for Am=0.1, Alpha=12.95, Rm=8.04

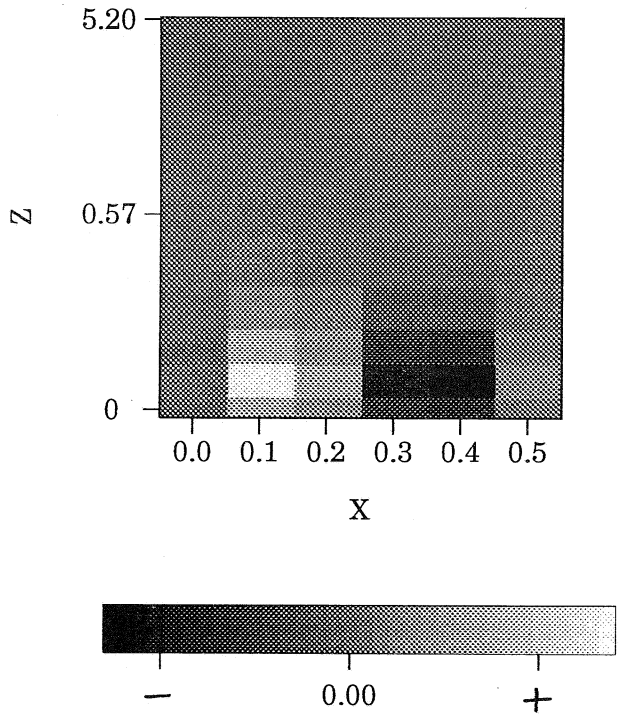

Figure 15

Perturbation of Solid Fraction for Am=0.3, Alpha=2.21, Rm=8.15

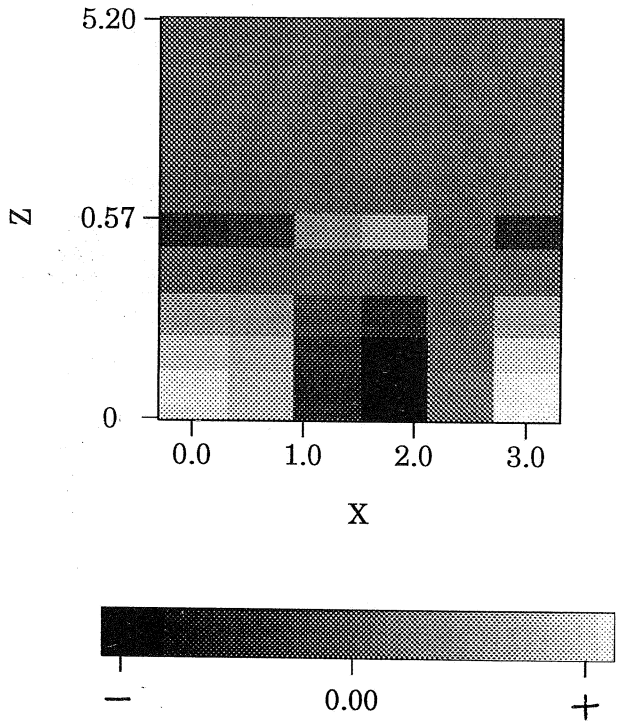

Figure 16

Perturbation of Solid Fraction for Am=0.3, Alpha=13.55, Rm=8.62

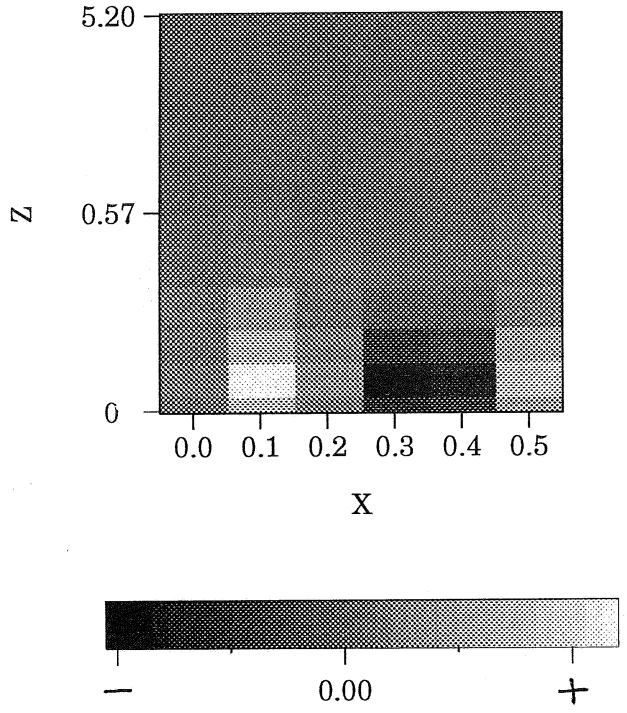

Figure 17

Perturbation of Solid Fraction for Am=0.6, Alpha=2.26, Rm=9.40

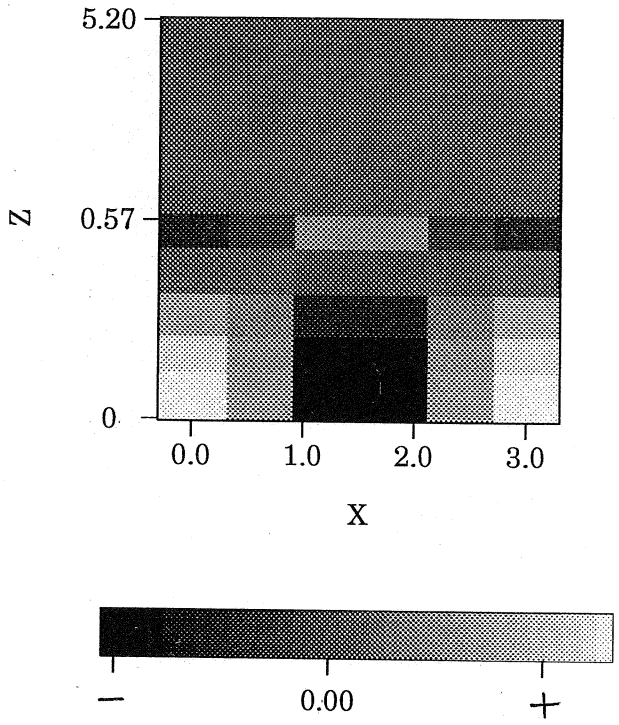

Figure 18

Perturbation of Solid Fraction for Am=0.6, Alpha=15.40, Rm=10.25

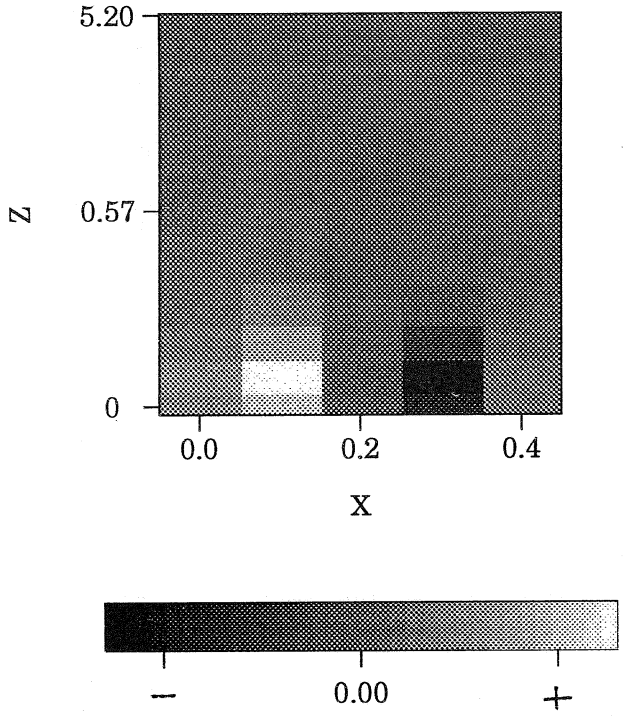

Figure 19

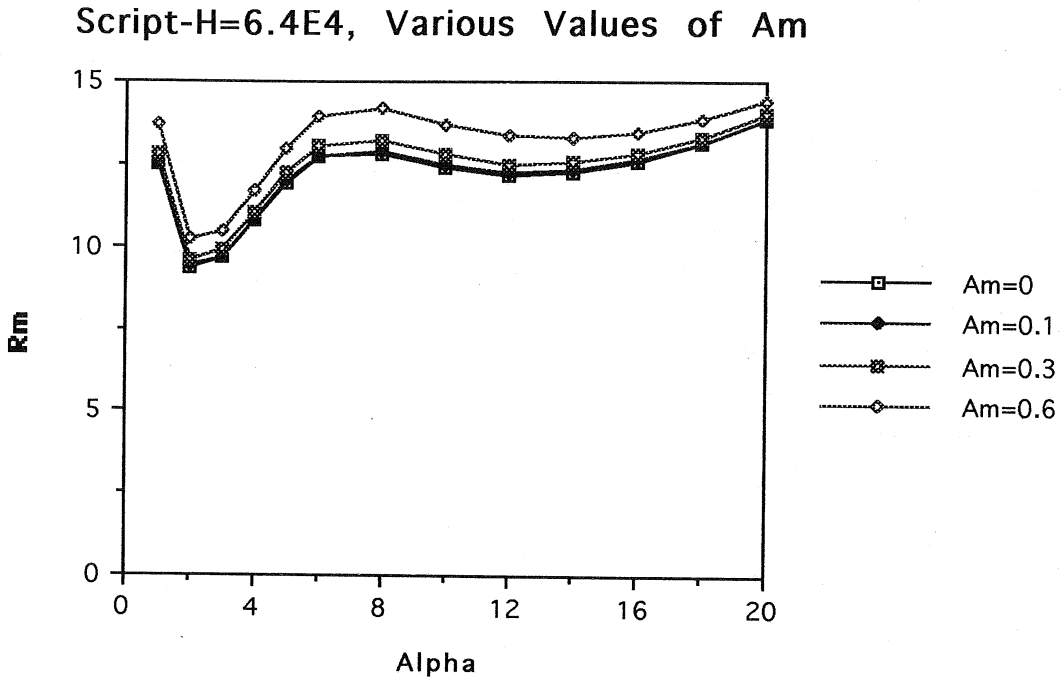

(a)

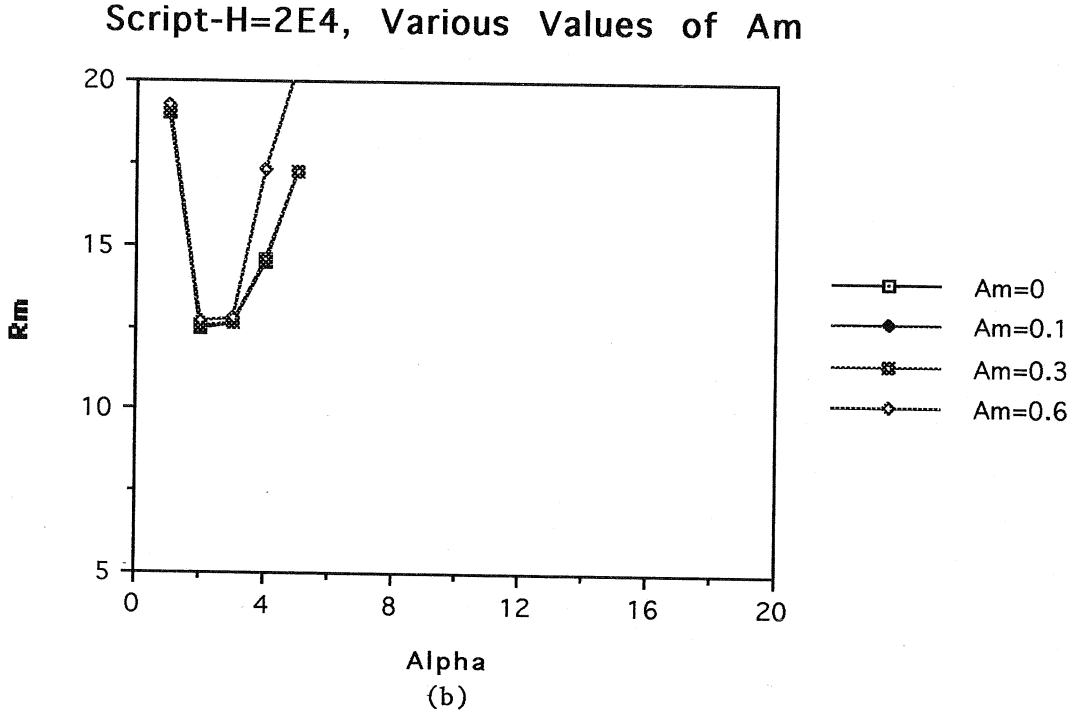

(b)

Figures 20

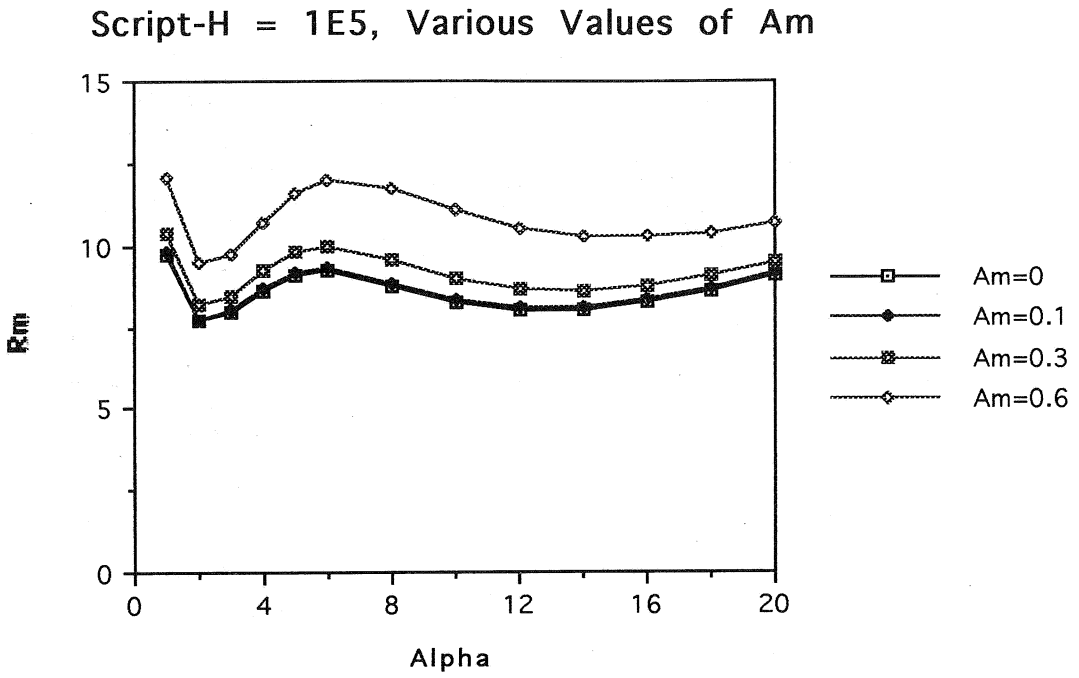

(a)

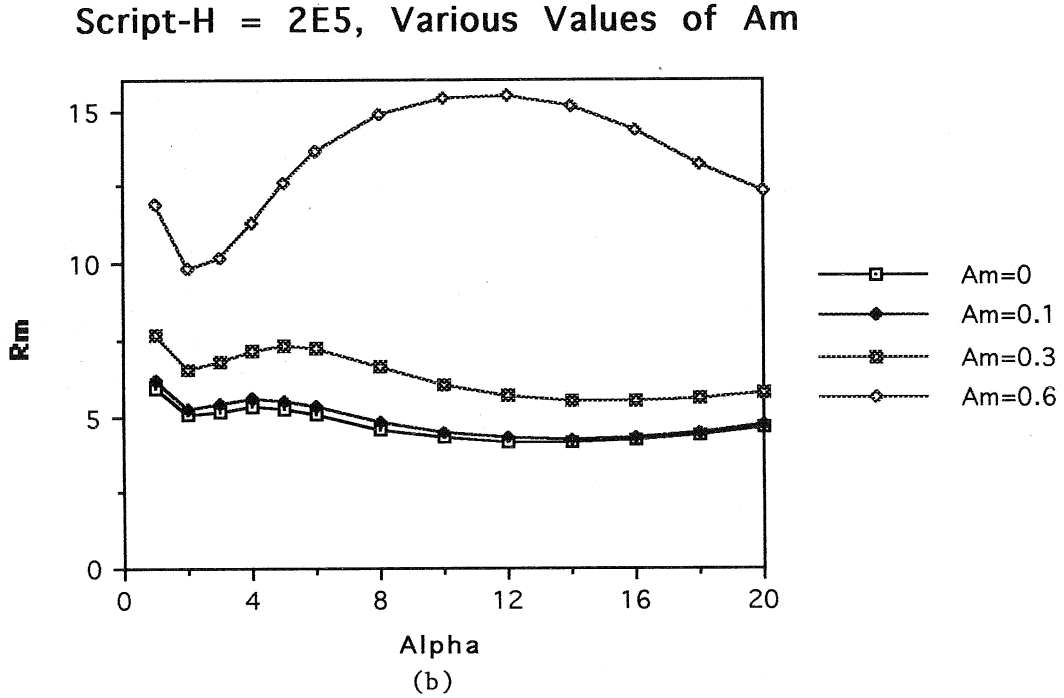

(b)

Figures 21

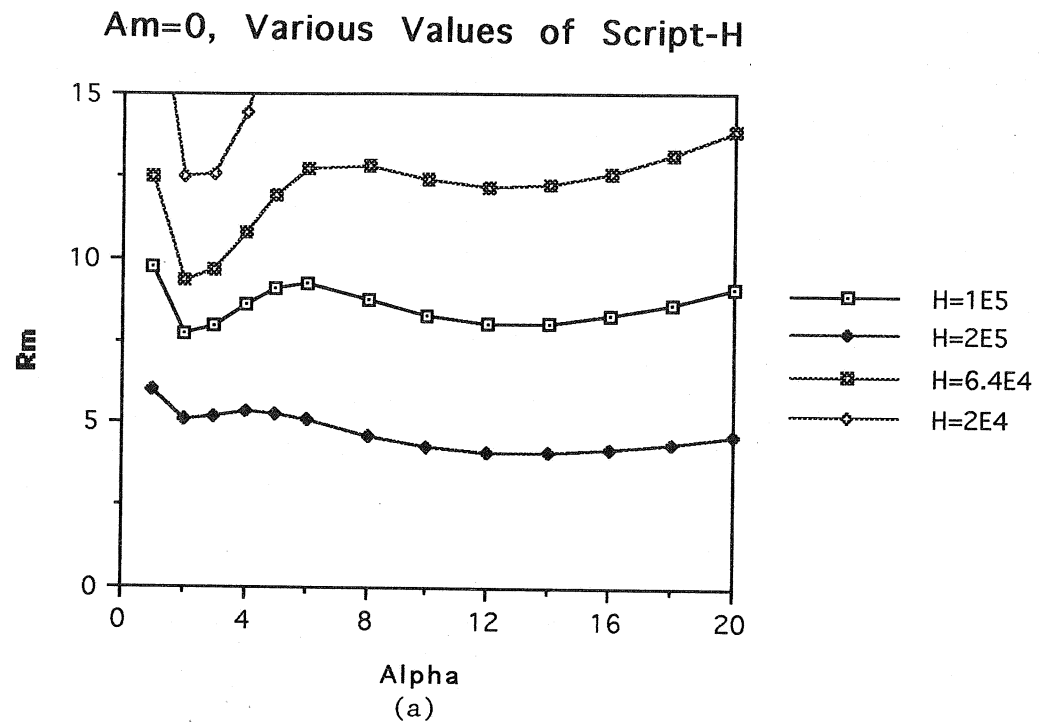

(a)

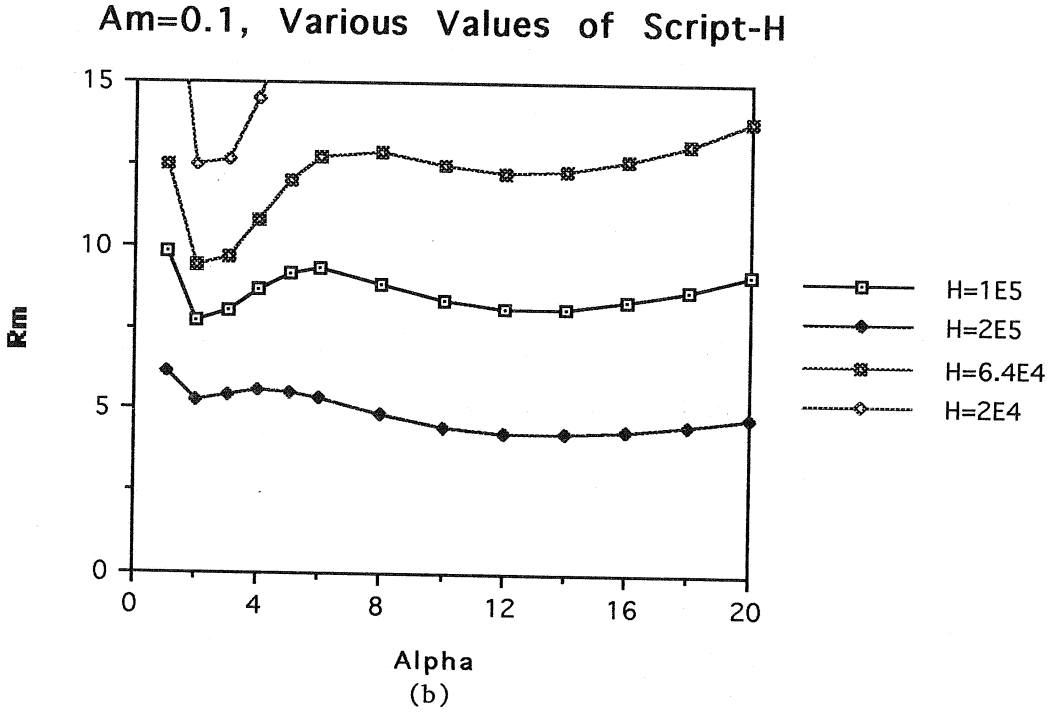

(b)

Figures 22

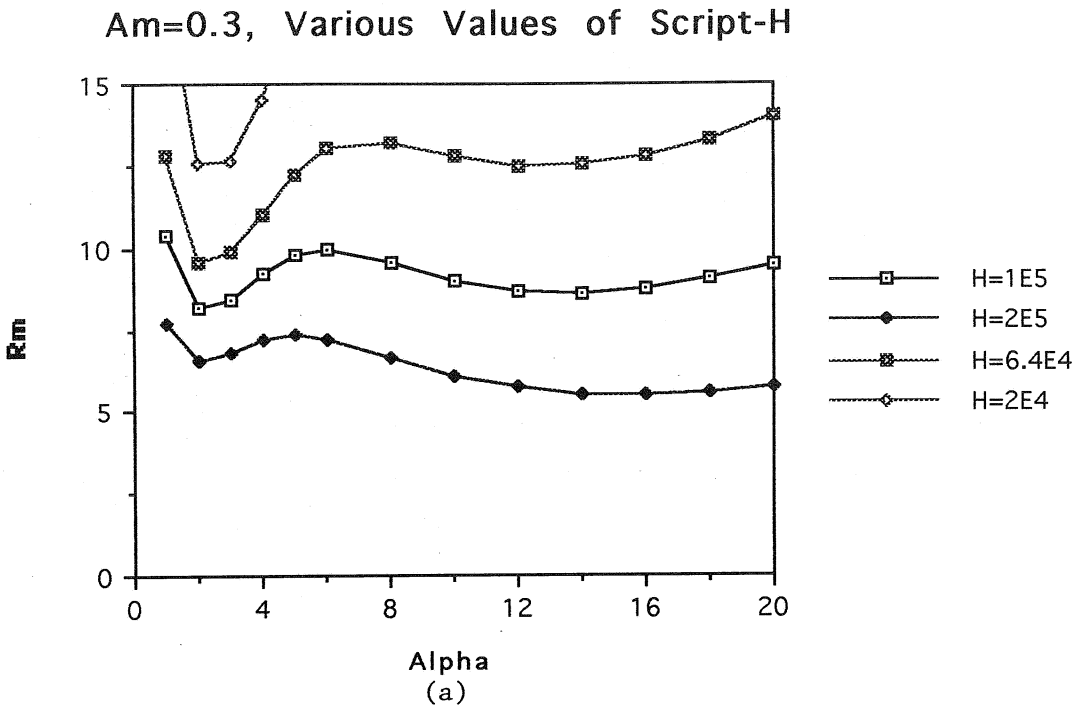

(a)

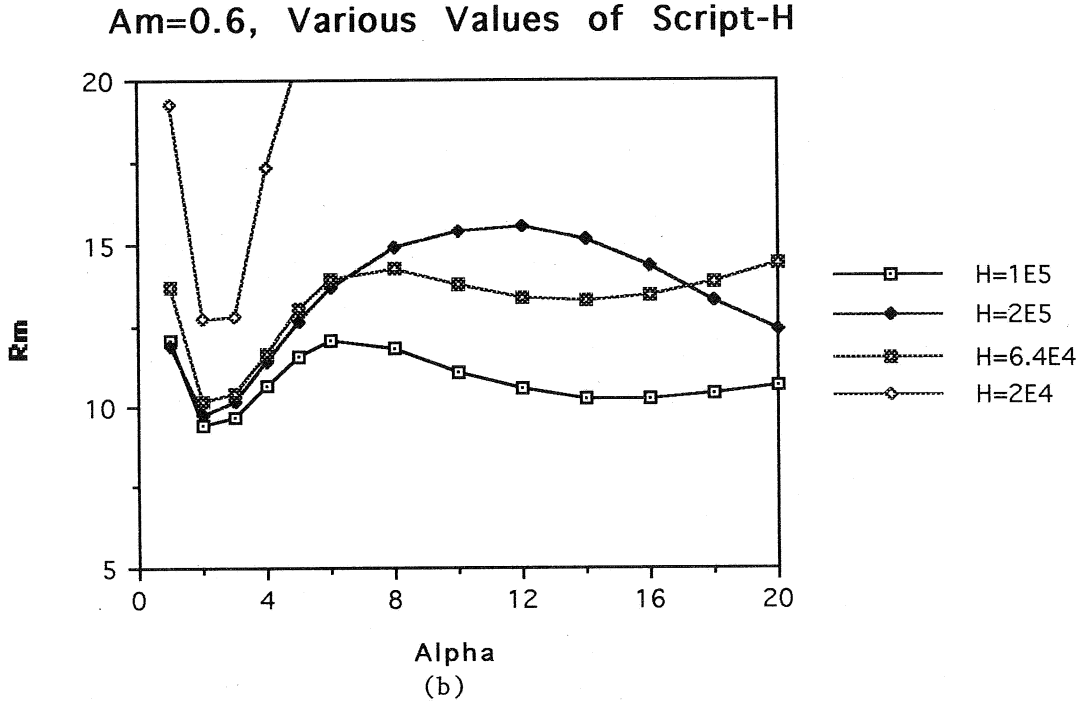

(b)

Figures 23

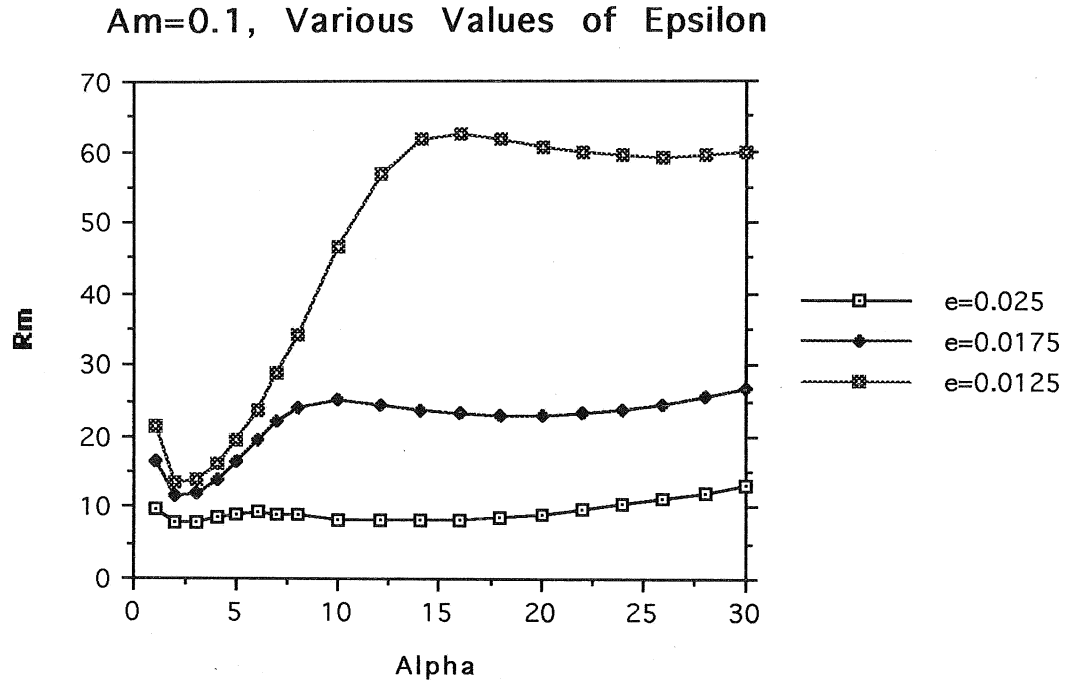

(a)

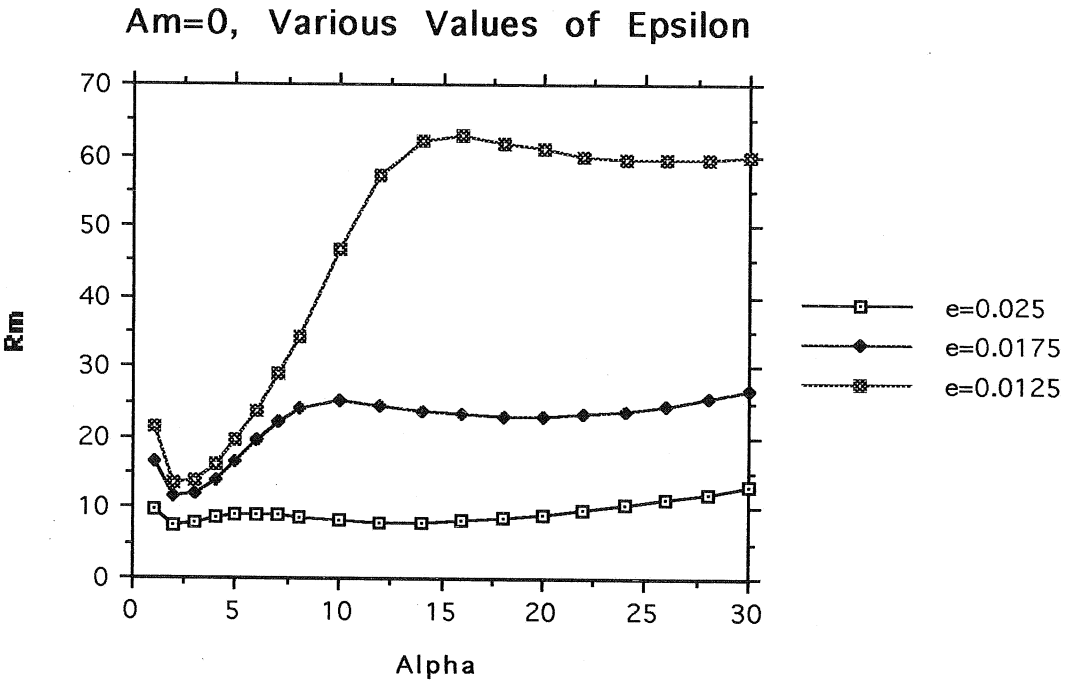

(b)

Figures 24

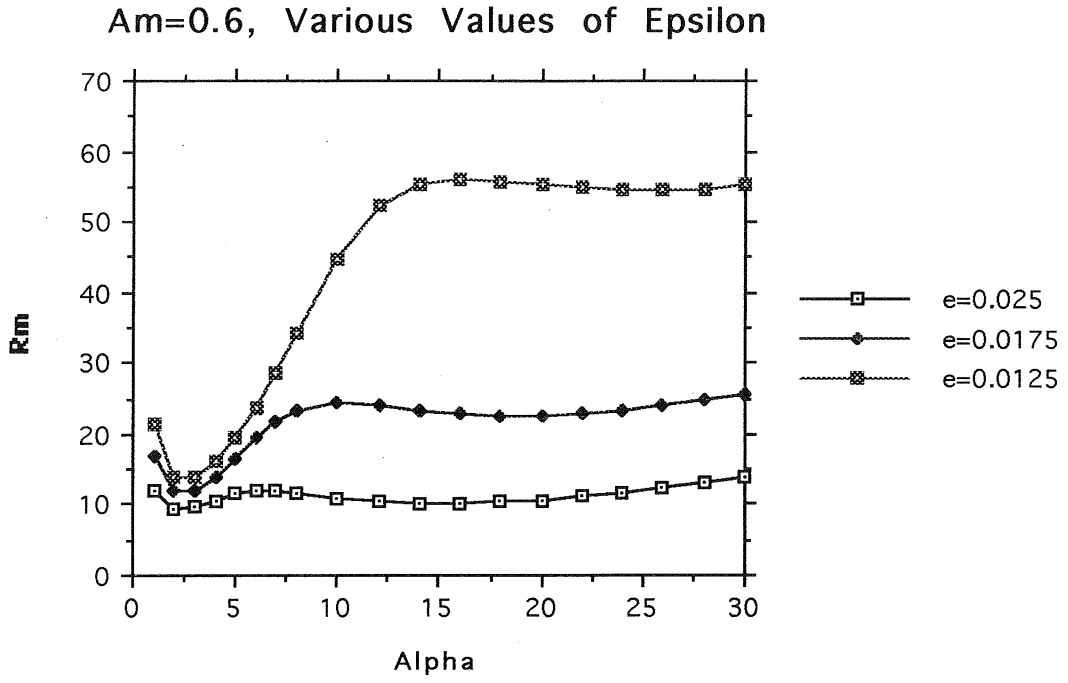

(a)

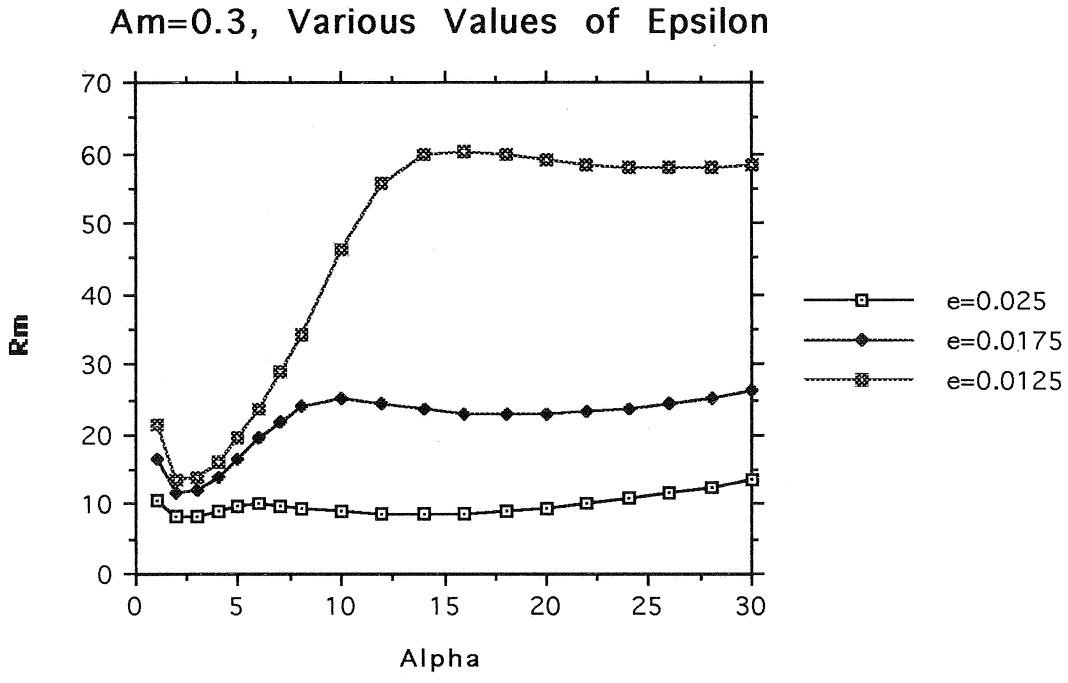

(b)

Figures 25

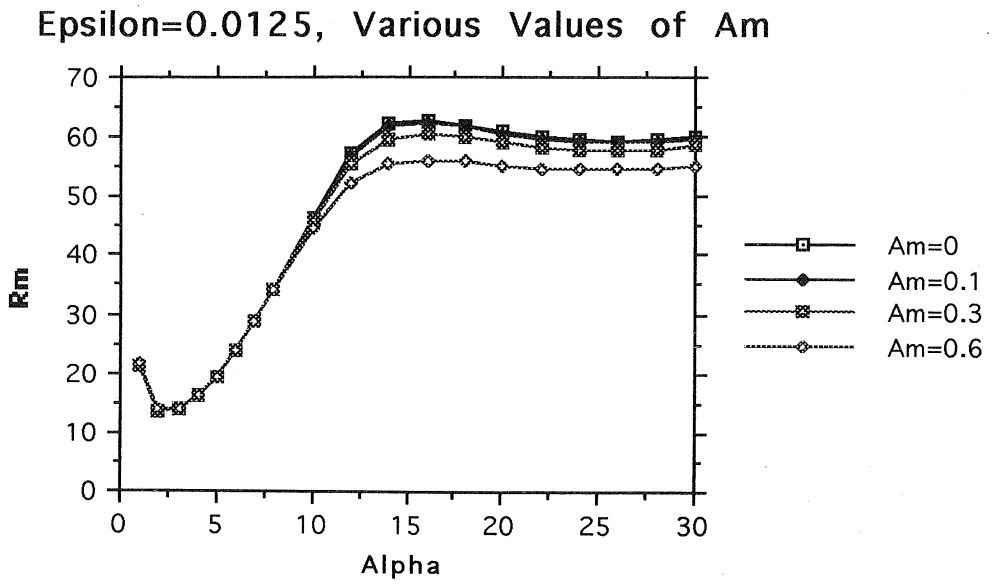

(a)

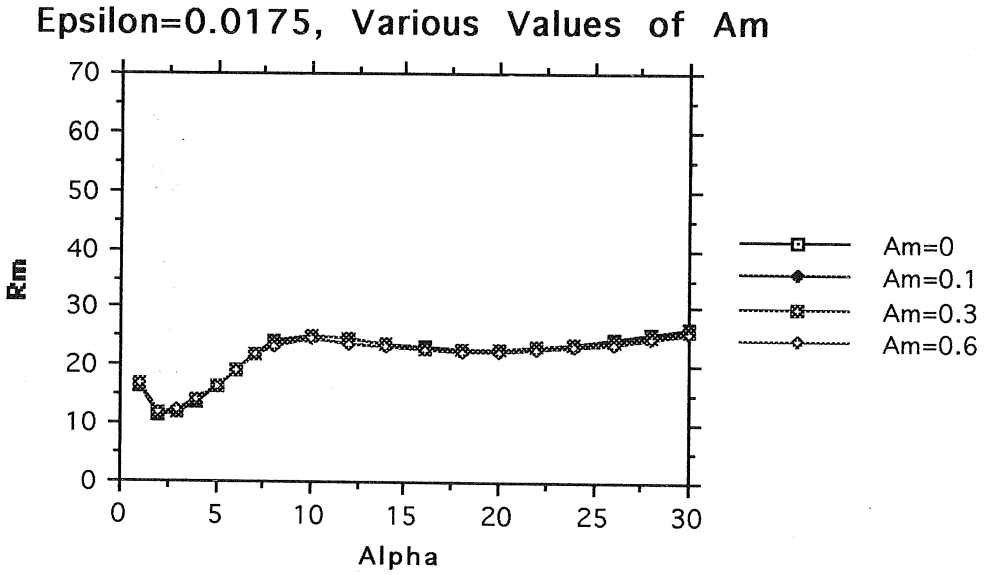

(b)

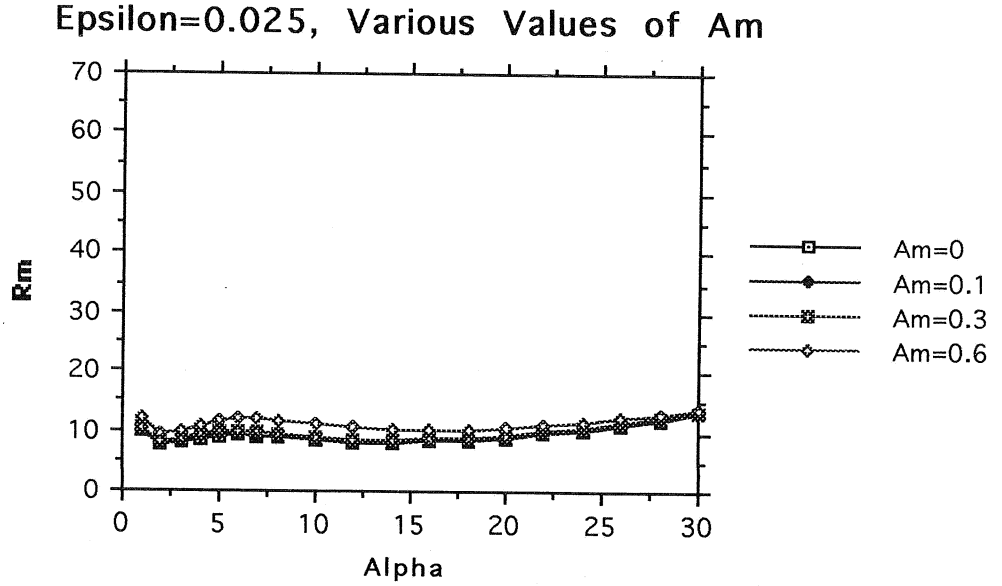

(c)

Figures 26

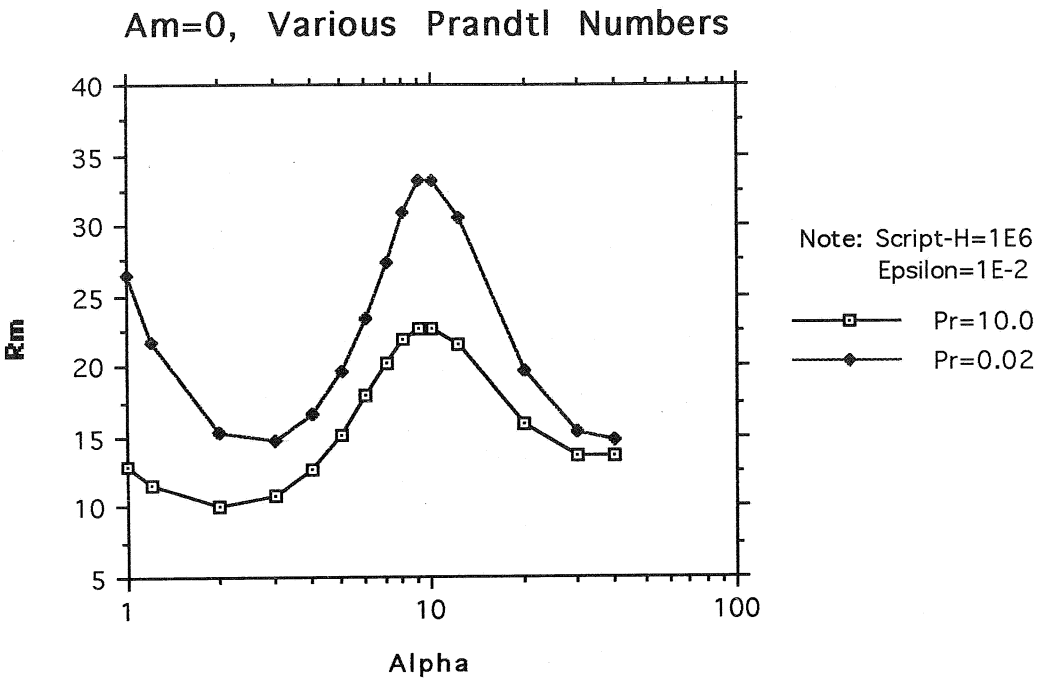

(a)

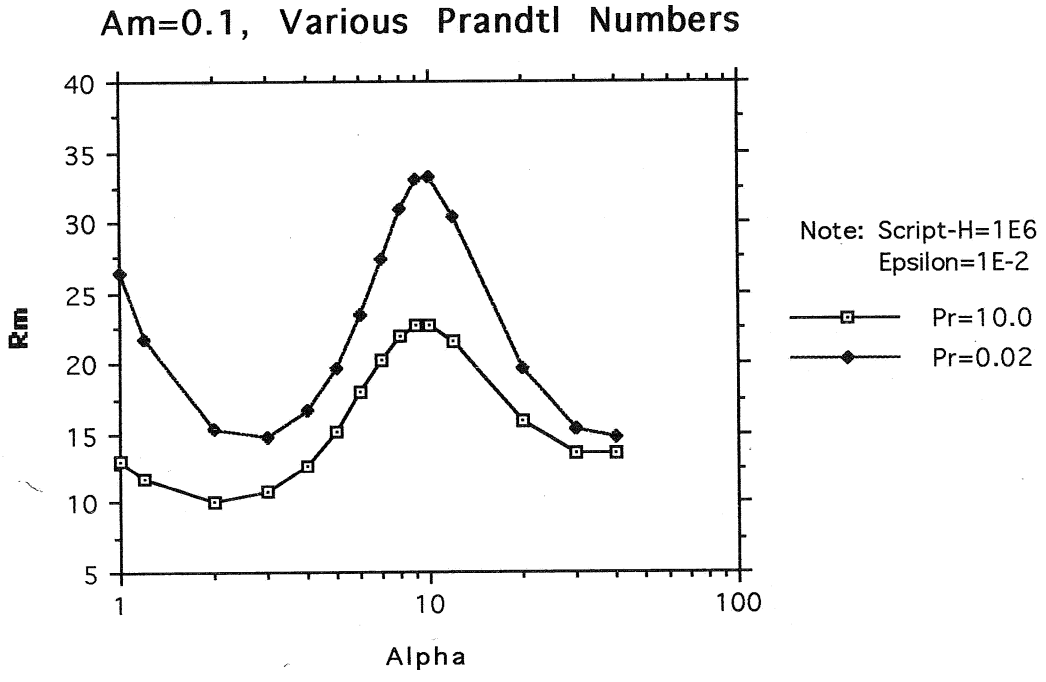

(b)

Figures 27

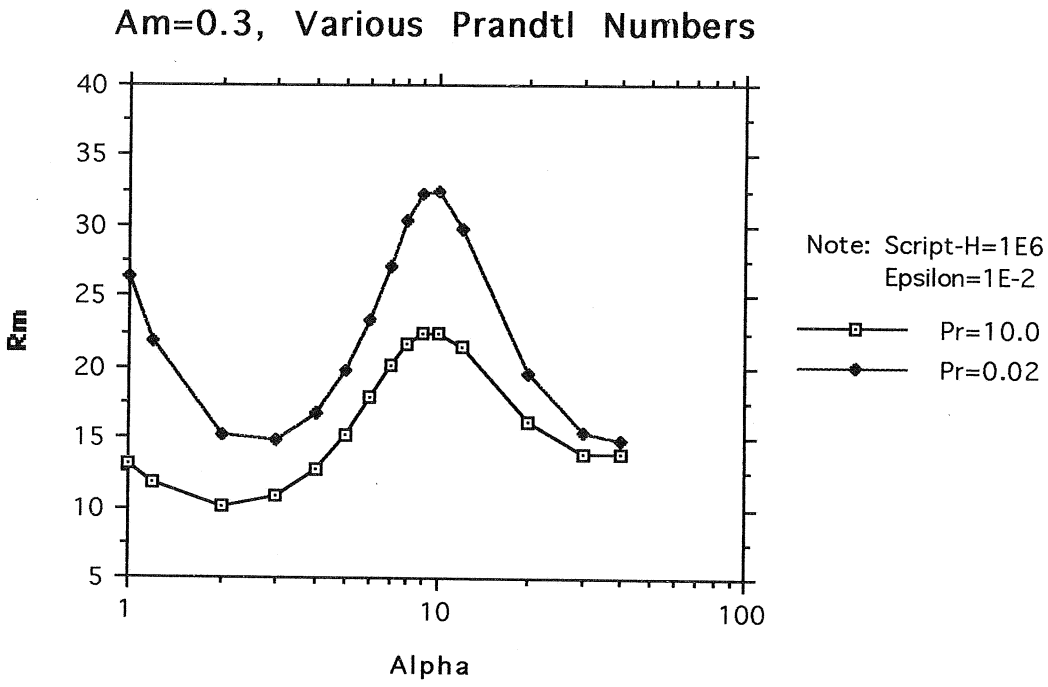

(a)

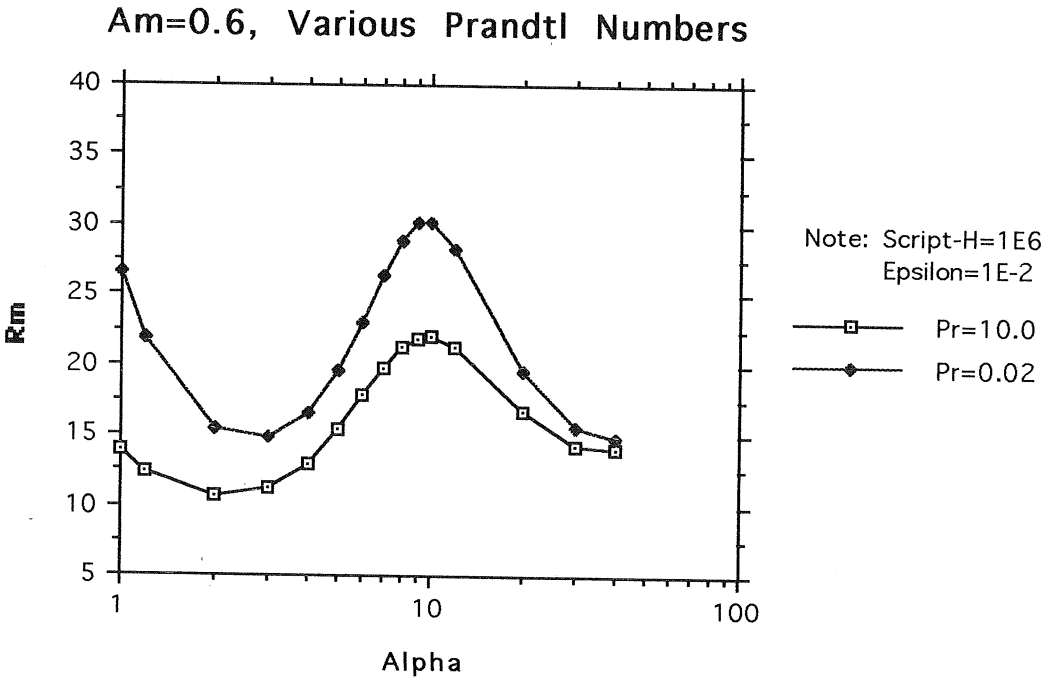

(b)

Figures 28

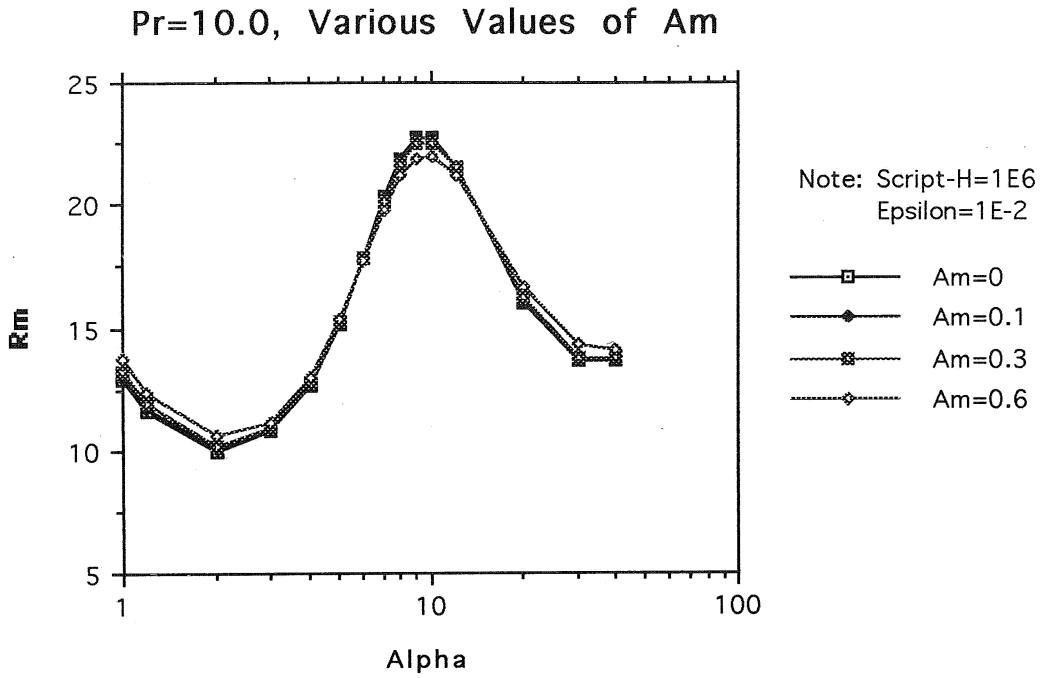

(a)

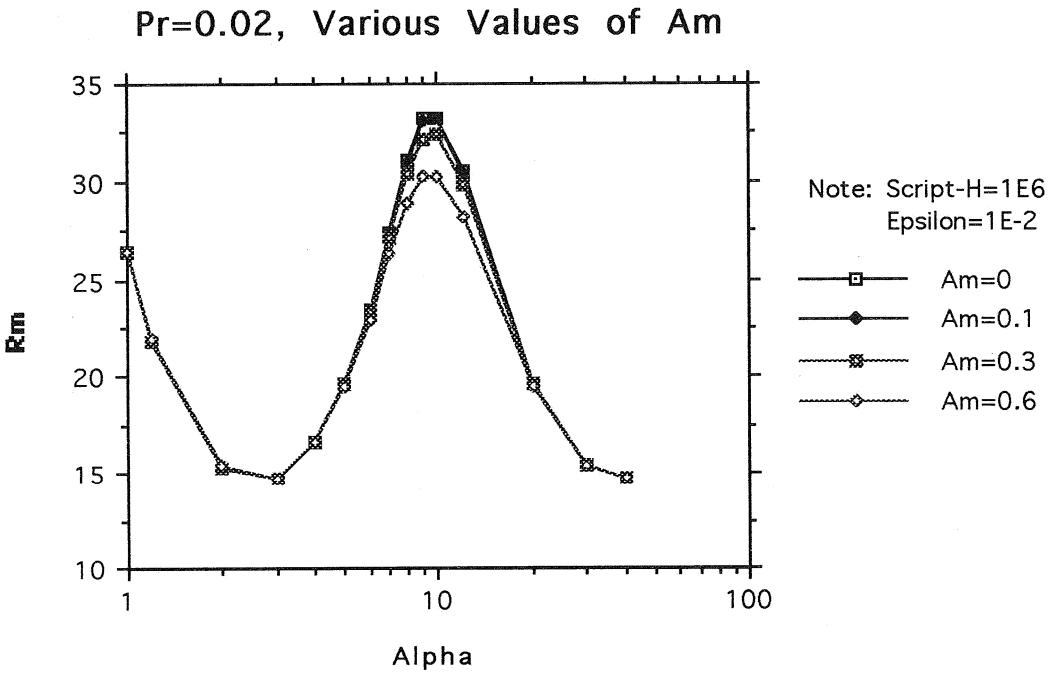

(b)

Figures 29

Am = .0 Al = .0E+00 Alpha = 2.19 Rm = 7.64 Wavelength = 2.87

For the liquid region:

Z = 5.20	X = .00	Re(W(X,Z)) = .87E-05	Re(U(X,Z)) = .00E+00
Z = 5.20	X = .60	Re(W(X,Z)) = .22E-05	Re(U(X,Z)) = .77E-05
Z = 5.20	X = 1.20	Re(W(X,Z)) = -.76E-05	Re(U(X,Z)) = .39E-05
Z = 5.20	X = 1.80	Re(W(X,Z)) = -.61E-05	Re(U(X,Z)) = -.57E-05
Z = 5.20	X = 2.40	Re(W(X,Z)) = .45E-05	Re(U(X,Z)) = -.68E-05
Z = 5.20	X = 3.00	Re(W(X,Z)) = .84E-05	Re(U(X,Z)) = .23E-05
Z = 2.21	X = .00	Re(W(X,Z)) = .23E-02	Re(U(X,Z)) = .00E+00
Z = 2.21	X = .60	Re(W(X,Z)) = .59E-03	Re(U(X,Z)) = .17E-02
Z = 2.21	X = 1.20	Re(W(X,Z)) = -.20E-02	Re(U(X,Z)) = .84E-03
Z = 2.21	X = 1.80	Re(W(X,Z)) = -.16E-02	Re(U(X,Z)) = -.12E-02
Z = 2.21	X = 2.40	Re(W(X,Z)) = .12E-02	Re(U(X,Z)) = -.15E-02
Z = 2.21	X = 3.00	Re(W(X,Z)) = .22E-02	Re(U(X,Z)) = .48E-03
Z = 1.52	X = .00	Re(W(X,Z)) = .63E-02	Re(U(X,Z)) = .00E+00
Z = 1.52	X = .60	Re(W(X,Z)) = .16E-02	Re(U(X,Z)) = .32E-02
Z = 1.52	X = 1.20	Re(W(X,Z)) = -.55E-02	Re(U(X,Z)) = .16E-02
Z = 1.52	X = 1.80	Re(W(X,Z)) = -.44E-02	Re(U(X,Z)) = -.24E-02
Z = 1.52	X = 2.40	Re(W(X,Z)) = .33E-02	Re(U(X,Z)) = -.29E-02
Z = 1.52	X = 3.00	Re(W(X,Z)) = .60E-02	Re(U(X,Z)) = .95E-03
Z = 1.11	X = .00	Re(W(X,Z)) = .89E-02	Re(U(X,Z)) = .00E+00
Z = 1.11	X = .60	Re(W(X,Z)) = .23E-02	Re(U(X,Z)) = .15E-02
Z = 1.11	X = 1.20	Re(W(X,Z)) = -.78E-02	Re(U(X,Z)) = .78E-03
Z = 1.11	X = 1.80	Re(W(X,Z)) = -.62E-02	Re(U(X,Z)) = -.11E-02
Z = 1.11	X = 2.40	Re(W(X,Z)) = .46E-02	Re(U(X,Z)) = -.14E-02
Z = 1.11	X = 3.00	Re(W(X,Z)) = .85E-02	Re(U(X,Z)) = .45E-03
Z = .82	X = .00	Re(W(X,Z)) = .80E-02	Re(U(X,Z)) = .00E+00
Z = .82	X = .60	Re(W(X,Z)) = .20E-02	Re(U(X,Z)) = -.58E-02
Z = .82	X = 1.20	Re(W(X,Z)) = -.70E-02	Re(U(X,Z)) = -.29E-02
Z = .82	X = 1.80	Re(W(X,Z)) = -.56E-02	Re(U(X,Z)) = .43E-02
Z = .82	X = 2.40	Re(W(X,Z)) = .41E-02	Re(U(X,Z)) = .51E-02
Z = .82	X = 3.00	Re(W(X,Z)) = .77E-02	Re(U(X,Z)) = -.17E-02
Z = .60	X = .00	Re(W(X,Z)) = .24E-02	Re(U(X,Z)) = .00E+00
Z = .60	X = .60	Re(W(X,Z)) = .62E-03	Re(U(X,Z)) = -.11E-01
Z = .60	X = 1.20	Re(W(X,Z)) = -.21E-02	Re(U(X,Z)) = -.57E-02
Z = .60	X = 1.80	Re(W(X,Z)) = -.17E-02	Re(U(X,Z)) = .83E-02
Z = .60	X = 2.40	Re(W(X,Z)) = .13E-02	Re(U(X,Z)) = .99E-02
Z = .60	X = 3.00	Re(W(X,Z)) = .23E-02	Re(U(X,Z)) = -.33E-02
Z = .57	X = .00	Re(W(X,Z)) = .21E-02	Re(U(X,Z)) = .00E+00
Z = .57	X = .60	Re(W(X,Z)) = .52E-03	Re(U(X,Z)) = .00E+00
Z = .57	X = 1.20	Re(W(X,Z)) = -.18E-02	Re(U(X,Z)) = .00E+00
Z = .57	X = 1.80	Re(W(X,Z)) = -.14E-02	Re(U(X,Z)) = .00E+00
Z = .57	X = 2.40	Re(W(X,Z)) = .11E-02	Re(U(X,Z)) = .00E+00
Z = .57	X = 3.00	Re(W(X,Z)) = .20E-02	Re(U(X,Z)) = .00E+00

For the mushy region:

Z = .57	X = .00	Re(W(X,Z)) = .21E-02	Re(U(X,Z)) = .00E+00
Z = .57	X = .60	Re(W(X,Z)) = .52E-03	Re(U(X,Z)) = -.28E-03
Z = .57	X = 1.20	Re(W(X,Z)) = -.18E-02	Re(U(X,Z)) = -.14E-03
Z = .57	X = 1.80	Re(W(X,Z)) = -.14E-02	Re(U(X,Z)) = .21E-03
Z = .57	X = 2.40	Re(W(X,Z)) = .11E-02	Re(U(X,Z)) = .25E-03
Z = .57	X = 3.00	Re(W(X,Z)) = .20E-02	Re(U(X,Z)) = -.81E-04
Z = .42	X = .00	Re(W(X,Z)) = .18E-02	Re(U(X,Z)) = .00E+00
Z = .42	X = .60	Re(W(X,Z)) = .46E-03	Re(U(X,Z)) = -.95E-03
Z = .42	X = 1.20	Re(W(X,Z)) = -.16E-02	Re(U(X,Z)) = -.48E-03
Z = .42	X = 1.80	Re(W(X,Z)) = -.13E-02	Re(U(X,Z)) = .71E-03
Z = .42	X = 2.40	Re(W(X,Z)) = .94E-03	Re(U(X,Z)) = .84E-03
Z = .42	X = 3.00	Re(W(X,Z)) = .18E-02	Re(U(X,Z)) = -.28E-03
Z = .29	X = .00	Re(W(X,Z)) = .14E-02	Re(U(X,Z)) = .00E+00
Z = .29	X = .60	Re(W(X,Z)) = .36E-03	Re(U(X,Z)) = -.14E-02
Z = .29	X = 1.20	Re(W(X,Z)) = -.12E-02	Re(U(X,Z)) = -.72E-03
Z = .29	X = 1.80	Re(W(X,Z)) = -.98E-03	Re(U(X,Z)) = .11E-02
Z = .29	X = 2.40	Re(W(X,Z)) = .73E-03	Re(U(X,Z)) = .13E-02
Z = .29	X = 3.00	Re(W(X,Z)) = .13E-02	Re(U(X,Z)) = -.42E-03
Z = .18	X = .00	Re(W(X,Z)) = .93E-03	Re(U(X,Z)) = .00E+00
Z = .18	X = .60	Re(W(X,Z)) = .24E-03	Re(U(X,Z)) = -.17E-02
Z = .18	X = 1.20	Re(W(X,Z)) = -.81E-03	Re(U(X,Z)) = -.87E-03
Z = .18	X = 1.80	Re(W(X,Z)) = -.65E-03	Re(U(X,Z)) = .13E-02
Z = .18	X = 2.40	Re(W(X,Z)) = .48E-03	Re(U(X,Z)) = .15E-02
Z = .18	X = 3.00	Re(W(X,Z)) = .89E-03	Re(U(X,Z)) = -.50E-03
Z = .09	X = .00	Re(W(X,Z)) = .45E-03	Re(U(X,Z)) = .00E+00
Z = .09	X = .60	Re(W(X,Z)) = .11E-03	Re(U(X,Z)) = -.19E-02
Z = .09	X = 1.20	Re(W(X,Z)) = -.39E-03	Re(U(X,Z)) = -.95E-03
Z = .09	X = 1.80	Re(W(X,Z)) = -.32E-03	Re(U(X,Z)) = .14E-02
Z = .09	X = 2.40	Re(W(X,Z)) = .23E-03	Re(U(X,Z)) = .16E-02
Z = .09	X = 3.00	Re(W(X,Z)) = .43E-03	Re(U(X,Z)) = -.54E-03
Z = .00	X = .00	Re(W(X,Z)) = .00E+00	Re(U(X,Z)) = .00E+00
Z = .00	X = .60	Re(W(X,Z)) = .00E+00	Re(U(X,Z)) = -.19E-02
Z = .00	X = 1.20	Re(W(X,Z)) = .00E+00	Re(U(X,Z)) = -.97E-03
Z = .00	X = 1.80	Re(W(X,Z)) = .00E+00	Re(U(X,Z)) = .14E-02
Z = .00	X = 2.40	Re(W(X,Z)) = .00E+00	Re(U(X,Z)) = .17E-02
Z = .00	X = 3.00	Re(W(X,Z)) = .00E+00	Re(U(X,Z)) = -.56E-03

Table 1

Am = .0 Al = .0E+00 Alpha = 12.93 Rm = 8.04 Wavelength = .49

For the liquid region:

Z = 5.20	X = .00	Re(W(X,Z)) = .28E-26	Re(U(X,Z)) = .00E+00
Z = 5.20	X = .10	Re(W(X,Z)) = .78E-27	Re(U(X,Z)) = .27E-26
Z = 5.20	X = .20	Re(W(X,Z)) = -.24E-26	Re(U(X,Z)) = .15E-26
Z = 5.20	X = .30	Re(W(X,Z)) = -.21E-26	Re(U(X,Z)) = -.19E-26
Z = 5.20	X = .40	Re(W(X,Z)) = .13E-26	Re(U(X,Z)) = -.25E-26
Z = 5.20	X = .50	Re(W(X,Z)) = .28E-26	Re(U(X,Z)) = .50E-27
Z = 2.21	X = .00	Re(W(X,Z)) = .66E-10	Re(U(X,Z)) = .00E+00
Z = 2.21	X = .10	Re(W(X,Z)) = .18E-10	Re(U(X,Z)) = .60E-10
Z = 2.21	X = .20	Re(W(X,Z)) = -.56E-10	Re(U(X,Z)) = .33E-10
Z = 2.21	X = .30	Re(W(X,Z)) = -.49E-10	Re(U(X,Z)) = -.42E-10
Z = 2.21	X = .40	Re(W(X,Z)) = .29E-10	Re(U(X,Z)) = -.56E-10
Z = 2.21	X = .50	Re(W(X,Z)) = .64E-10	Re(U(X,Z)) = .11E-10
Z = 1.52	X = .00	Re(W(X,Z)) = .30E-06	Re(U(X,Z)) = .00E+00
Z = 1.52	X = .10	Re(W(X,Z)) = .83E-07	Re(U(X,Z)) = .27E-06
Z = 1.52	X = .20	Re(W(X,Z)) = -.26E-06	Re(U(X,Z)) = .15E-06
Z = 1.52	X = .30	Re(W(X,Z)) = -.22E-06	Re(U(X,Z)) = -.19E-06
Z = 1.52	X = .40	Re(W(X,Z)) = .13E-06	Re(U(X,Z)) = -.25E-06
Z = 1.52	X = .50	Re(W(X,Z)) = .30E-06	Re(U(X,Z)) = .50E-07
Z = 1.11	X = .00	Re(W(X,Z)) = .32E-04	Re(U(X,Z)) = .00E+00
Z = 1.11	X = .10	Re(W(X,Z)) = .87E-05	Re(U(X,Z)) = .26E-04
Z = 1.11	X = .20	Re(W(X,Z)) = -.27E-04	Re(U(X,Z)) = .14E-04
Z = 1.11	X = .30	Re(W(X,Z)) = -.23E-04	Re(U(X,Z)) = -.18E-04
Z = 1.11	X = .40	Re(W(X,Z)) = .14E-04	Re(U(X,Z)) = -.24E-04
Z = 1.11	X = .50	Re(W(X,Z)) = .31E-04	Re(U(X,Z)) = .48E-05
Z = .82	X = .00	Re(W(X,Z)) = .53E-03	Re(U(X,Z)) = .00E+00
Z = .82	X = .10	Re(W(X,Z)) = .15E-03	Re(U(X,Z)) = .31E-03
Z = .82	X = .20	Re(W(X,Z)) = -.45E-03	Re(U(X,Z)) = .17E-03
Z = .82	X = .30	Re(W(X,Z)) = -.39E-03	Re(U(X,Z)) = -.22E-03
Z = .82	X = .40	Re(W(X,Z)) = .24E-03	Re(U(X,Z)) = -.29E-03
Z = .82	X = .50	Re(W(X,Z)) = .52E-03	Re(U(X,Z)) = .58E-04
Z = .60	X = .00	Re(W(X,Z)) = .23E-03	Re(U(X,Z)) = .00E+00
Z = .60	X = .10	Re(W(X,Z)) = .64E-04	Re(U(X,Z)) = -.93E-03
Z = .60	X = .20	Re(W(X,Z)) = -.20E-03	Re(U(X,Z)) = -.51E-03
Z = .60	X = .30	Re(W(X,Z)) = -.17E-03	Re(U(X,Z)) = .65E-03
Z = .60	X = .40	Re(W(X,Z)) = .10E-03	Re(U(X,Z)) = .86E-03
Z = .60	X = .50	Re(W(X,Z)) = .23E-03	Re(U(X,Z)) = -.17E-03
Z = .57	X = .00	Re(W(X,Z)) = .32E-04	Re(U(X,Z)) = .00E+00
Z = .57	X = .10	Re(W(X,Z)) = .89E-05	Re(U(X,Z)) = -.17E-14
Z = .57	X = .20	Re(W(X,Z)) = -.27E-04	Re(U(X,Z)) = -.94E-15
Z = .57	X = .30	Re(W(X,Z)) = -.24E-04	Re(U(X,Z)) = .12E-14
Z = .57	X = .40	Re(W(X,Z)) = .14E-04	Re(U(X,Z)) = .16E-14
Z = .57	X = .50	Re(W(X,Z)) = .32E-04	Re(U(X,Z)) = -.32E-15

For the mushy region:

Z = .57	X = .00	Re(W(X,Z)) = .32E-04	Re(U(X,Z)) = .00E+00
Z = .57	X = .10	Re(W(X,Z)) = .89E-05	Re(U(X,Z)) = -.24E-04
Z = .57	X = .20	Re(W(X,Z)) = -.27E-04	Re(U(X,Z)) = -.13E-04
Z = .57	X = .30	Re(W(X,Z)) = -.24E-04	Re(U(X,Z)) = .17E-04
Z = .57	X = .40	Re(W(X,Z)) = .14E-04	Re(U(X,Z)) = .22E-04
Z = .57	X = .50	Re(W(X,Z)) = .32E-04	Re(U(X,Z)) = -.45E-05
Z = .42	X = .00	Re(W(X,Z)) = .66E-05	Re(U(X,Z)) = .00E+00
Z = .42	X = .10	Re(W(X,Z)) = .18E-05	Re(U(X,Z)) = -.55E-05
Z = .42	X = .20	Re(W(X,Z)) = -.56E-05	Re(U(X,Z)) = -.30E-05
Z = .42	X = .30	Re(W(X,Z)) = -.49E-05	Re(U(X,Z)) = .39E-05
Z = .42	X = .40	Re(W(X,Z)) = .29E-05	Re(U(X,Z)) = .52E-05
Z = .42	X = .50	Re(W(X,Z)) = .65E-05	Re(U(X,Z)) = -.10E-05
Z = .29	X = .00	Re(W(X,Z)) = -.92E-06	Re(U(X,Z)) = .00E+00
Z = .29	X = .10	Re(W(X,Z)) = -.25E-06	Re(U(X,Z)) = -.28E-05
Z = .29	X = .20	Re(W(X,Z)) = .78E-06	Re(U(X,Z)) = -.15E-05
Z = .29	X = .30	Re(W(X,Z)) = .68E-06	Re(U(X,Z)) = .19E-05
Z = .29	X = .40	Re(W(X,Z)) = -.41E-06	Re(U(X,Z)) = .26E-05
Z = .29	X = .50	Re(W(X,Z)) = -.91E-06	Re(U(X,Z)) = -.52E-06
Z = .18	X = .00	Re(W(X,Z)) = -.62E-05	Re(U(X,Z)) = .00E+00
Z = .18	X = .10	Re(W(X,Z)) = -.17E-05	Re(U(X,Z)) = -.33E-05
Z = .18	X = .20	Re(W(X,Z)) = .53E-05	Re(U(X,Z)) = -.18E-05
Z = .18	X = .30	Re(W(X,Z)) = .46E-05	Re(U(X,Z)) = .23E-05
Z = .18	X = .40	Re(W(X,Z)) = -.28E-05	Re(U(X,Z)) = .30E-05
Z = .18	X = .50	Re(W(X,Z)) = -.61E-05	Re(U(X,Z)) = -.61E-06
Z = .09	X = .00	Re(W(X,Z)) = -.10E-04	Re(U(X,Z)) = .00E+00
Z = .09	X = .10	Re(W(X,Z)) = -.29E-05	Re(U(X,Z)) = -.77E-06
Z = .09	X = .20	Re(W(X,Z)) = .89E-05	Re(U(X,Z)) = -.42E-06
Z = .09	X = .30	Re(W(X,Z)) = .78E-05	Re(U(X,Z)) = .54E-06
Z = .09	X = .40	Re(W(X,Z)) = -.47E-05	Re(U(X,Z)) = .72E-06
Z = .09	X = .50	Re(W(X,Z)) = -.10E-04	Re(U(X,Z)) = -.14E-06
Z = .00	X = .00	Re(W(X,Z)) = .91E-12	Re(U(X,Z)) = .00E+00
Z = .00	X = .10	Re(W(X,Z)) = .25E-12	Re(U(X,Z)) = .22E-04
Z = .00	X = .20	Re(W(X,Z)) = -.77E-12	Re(U(X,Z)) = .12E-04
Z = .00	X = .30	Re(W(X,Z)) = -.67E-12	Re(U(X,Z)) = -.16E-04
Z = .00	X = .40	Re(W(X,Z)) = .40E-12	Re(U(X,Z)) = -.21E-04
Z = .00	X = .50	Re(W(X,Z)) = .89E-12	Re(U(X,Z)) = .42E-05

Table 2

Am = .1 Al = .1E+05 Alpha = 2.20 Rm = 7.71 Wavelength = 2.86

For the liquid region:

Z = 5.20	X = .00	Re(W(X,Z)) = .81E-05	Re(U(X,Z)) = .41E-06
Z = 5.20	X = .60	Re(W(X,Z)) = .16E-05	Re(U(X,Z)) = .72E-05
Z = 5.20	X = 1.20	Re(W(X,Z)) = -.73E-05	Re(U(X,Z)) = .32E-05
Z = 5.20	X = 1.80	Re(W(X,Z)) = -.52E-05	Re(U(X,Z)) = -.56E-05
Z = 5.20	X = 2.40	Re(W(X,Z)) = .47E-05	Re(U(X,Z)) = -.60E-05
Z = 5.20	X = 3.00	Re(W(X,Z)) = .75E-05	Re(U(X,Z)) = .27E-05
Z = 2.21	X = .00	Re(W(X,Z)) = .21E-02	Re(U(X,Z)) = .34E-03
Z = 2.21	X = .60	Re(W(X,Z)) = .19E-03	Re(U(X,Z)) = .15E-02
Z = 2.21	X = 1.20	Re(W(X,Z)) = -.20E-02	Re(U(X,Z)) = .40E-03
Z = 2.21	X = 1.80	Re(W(X,Z)) = -.12E-02	Re(U(X,Z)) = -.13E-02
Z = 2.21	X = 2.40	Re(W(X,Z)) = .14E-02	Re(U(X,Z)) = -.10E-02
Z = 2.21	X = 3.00	Re(W(X,Z)) = .19E-02	Re(U(X,Z)) = .78E-03
Z = 1.52	X = .00	Re(W(X,Z)) = .52E-02	Re(U(X,Z)) = .17E-02
Z = 1.52	X = .60	Re(W(X,Z)) = -.28E-03	Re(U(X,Z)) = .26E-02
Z = 1.52	X = 1.20	Re(W(X,Z)) = -.53E-02	Re(U(X,Z)) = -.36E-03
Z = 1.52	X = 1.80	Re(W(X,Z)) = -.24E-02	Re(U(X,Z)) = -.28E-02
Z = 1.52	X = 2.40	Re(W(X,Z)) = .41E-02	Re(U(X,Z)) = -.10E-02
Z = 1.52	X = 3.00	Re(W(X,Z)) = .44E-02	Re(U(X,Z)) = .23E-02
Z = 1.11	X = .00	Re(W(X,Z)) = .62E-02	Re(U(X,Z)) = .41E-02
Z = 1.11	X = .60	Re(W(X,Z)) = -.24E-02	Re(U(X,Z)) = -.23E-04
Z = 1.11	X = 1.20	Re(W(X,Z)) = -.74E-02	Re(U(X,Z)) = -.41E-02
Z = 1.11	X = 1.80	Re(W(X,Z)) = -.13E-02	Re(U(X,Z)) = -.20E-02
Z = 1.11	X = 2.40	Re(W(X,Z)) = .67E-02	Re(U(X,Z)) = .31E-02
Z = 1.11	X = 3.00	Re(W(X,Z)) = .47E-02	Re(U(X,Z)) = .36E-02
Z = .82	X = .00	Re(W(X,Z)) = .29E-02	Re(U(X,Z)) = .79E-02
Z = .82	X = .60	Re(W(X,Z)) = -.67E-02	Re(U(X,Z)) = -.87E-02
Z = .82	X = 1.20	Re(W(X,Z)) = -.63E-02	Re(U(X,Z)) = -.12E-01
Z = .82	X = 1.80	Re(W(X,Z)) = .36E-02	Re(U(X,Z)) = .27E-02
Z = .82	X = 2.40	Re(W(X,Z)) = .81E-02	Re(U(X,Z)) = .14E-01
Z = .82	X = 3.00	Re(W(X,Z)) = .40E-03	Re(U(X,Z)) = .41E-02
Z = .60	X = .00	Re(W(X,Z)) = -.60E-02	Re(U(X,Z)) = .11E-01
Z = .60	X = .60	Re(W(X,Z)) = -.14E-01	Re(U(X,Z)) = -.16E-01
Z = .60	X = 1.20	Re(W(X,Z)) = -.88E-03	Re(U(X,Z)) = -.19E-01
Z = .60	X = 1.80	Re(W(X,Z)) = .13E-01	Re(U(X,Z)) = .70E-02
Z = .60	X = 2.40	Re(W(X,Z)) = .75E-02	Re(U(X,Z)) = .22E-01
Z = .60	X = 3.00	Re(W(X,Z)) = -.96E-02	Re(U(X,Z)) = .40E-02
Z = .57	X = .00	Re(W(X,Z)) = -.67E-02	Re(U(X,Z)) = -.89E-15
Z = .57	X = .60	Re(W(X,Z)) = -.14E-01	Re(U(X,Z)) = -.22E-15
Z = .57	X = 1.20	Re(W(X,Z)) = -.46E-03	Re(U(X,Z)) = .78E-15
Z = .57	X = 1.80	Re(W(X,Z)) = .14E-01	Re(U(X,Z)) = .61E-15
Z = .57	X = 2.40	Re(W(X,Z)) = .75E-02	Re(U(X,Z)) = -.48E-15
Z = .57	X = 3.00	Re(W(X,Z)) = -.10E-01	Re(U(X,Z)) = -.84E-15

For the mushy region:

Z = .57	X = .00	Re(W(X,Z)) = -.67E-02	Re(U(X,Z)) = .43E-03
Z = .57	X = .60	Re(W(X,Z)) = -.14E-01	Re(U(X,Z)) = -.54E-03
Z = .57	X = 1.20	Re(W(X,Z)) = -.46E-03	Re(U(X,Z)) = -.70E-03
Z = .57	X = 1.80	Re(W(X,Z)) = .14E-01	Re(U(X,Z)) = .19E-03
Z = .57	X = 2.40	Re(W(X,Z)) = .75E-02	Re(U(X,Z)) = .80E-03
Z = .57	X = 3.00	Re(W(X,Z)) = -.10E-01	Re(U(X,Z)) = .20E-03
Z = .42	X = .00	Re(W(X,Z)) = -.67E-02	Re(U(X,Z)) = -.28E-02
Z = .42	X = .60	Re(W(X,Z)) = -.14E-01	Re(U(X,Z)) = .87E-04
Z = .42	X = 1.20	Re(W(X,Z)) = -.27E-03	Re(U(X,Z)) = .28E-02
Z = .42	X = 1.80	Re(W(X,Z)) = .14E-01	Re(U(X,Z)) = .13E-02
Z = .42	X = 2.40	Re(W(X,Z)) = .72E-02	Re(U(X,Z)) = -.22E-02
Z = .42	X = 3.00	Re(W(X,Z)) = -.10E-01	Re(U(X,Z)) = -.24E-02
Z = .29	X = .00	Re(W(X,Z)) = -.60E-02	Re(U(X,Z)) = -.71E-02
Z = .29	X = .60	Re(W(X,Z)) = -.12E-01	Re(U(X,Z)) = .14E-02
Z = .29	X = 1.20	Re(W(X,Z)) = -.56E-04	Re(U(X,Z)) = .78E-02
Z = .29	X = 1.80	Re(W(X,Z)) = .12E-01	Re(U(X,Z)) = .25E-02
Z = .29	X = 2.40	Re(W(X,Z)) = .61E-02	Re(U(X,Z)) = -.65E-02
Z = .29	X = 3.00	Re(W(X,Z)) = -.92E-02	Re(U(X,Z)) = -.57E-02
Z = .18	X = .00	Re(W(X,Z)) = -.47E-02	Re(U(X,Z)) = -.12E-01
Z = .18	X = .60	Re(W(X,Z)) = -.92E-02	Re(U(X,Z)) = .30E-02
Z = .18	X = 1.20	Re(W(X,Z)) = .80E-04	Re(U(X,Z)) = .13E-01
Z = .18	X = 1.80	Re(W(X,Z)) = .93E-02	Re(U(X,Z)) = .36E-02
Z = .18	X = 2.40	Re(W(X,Z)) = .45E-02	Re(U(X,Z)) = -.12E-01
Z = .18	X = 3.00	Re(W(X,Z)) = -.70E-02	Re(U(X,Z)) = -.93E-02
Z = .09	X = .00	Re(W(X,Z)) = -.27E-02	Re(U(X,Z)) = -.17E-01
Z = .09	X = .60	Re(W(X,Z)) = -.51E-02	Re(U(X,Z)) = .50E-02
Z = .09	X = 1.20	Re(W(X,Z)) = .11E-03	Re(U(X,Z)) = .20E-01
Z = .09	X = 1.80	Re(W(X,Z)) = .52E-02	Re(U(X,Z)) = .47E-02
Z = .09	X = 2.40	Re(W(X,Z)) = .25E-02	Re(U(X,Z)) = -.17E-01
Z = .09	X = 3.00	Re(W(X,Z)) = -.40E-02	Re(U(X,Z)) = -.13E-01
Z = .00	X = .00	Re(W(X,Z)) = .00E+00	Re(U(X,Z)) = -.23E-01
Z = .00	X = .60	Re(W(X,Z)) = .48E-15	Re(U(X,Z)) = .74E-02
Z = .00	X = 1.20	Re(W(X,Z)) = .24E-15	Re(U(X,Z)) = .27E-01
Z = .00	X = 1.80	Re(W(X,Z)) = -.36E-15	Re(U(X,Z)) = .58E-02
Z = .00	X = 2.40	Re(W(X,Z)) = -.42E-15	Re(U(X,Z)) = -.24E-01
Z = .00	X = 3.00	Re(W(X,Z)) = .16E-15	Re(U(X,Z)) = -.18E-01

Table 3

Am = .1 Al = .1E+05 Alpha = 12.95 Rm = 8.04 Wavelength = .49

For the liquid region:

Z = 5.20	X = .00	Re(W(X,Z)) = .26E-26	Re(U(X,Z)) = .25E-29
Z = 5.20	X = .10	Re(W(X,Z)) = .70E-27	Re(U(X,Z)) = .24E-26
Z = 5.20	X = .20	Re(W(X,Z)) = -.22E-26	Re(U(X,Z)) = .13E-26
Z = 5.20	X = .30	Re(W(X,Z)) = -.19E-26	Re(U(X,Z)) = -.17E-26
Z = 5.20	X = .40	Re(W(X,Z)) = .12E-26	Re(U(X,Z)) = -.23E-26
Z = 5.20	X = .50	Re(W(X,Z)) = .25E-26	Re(U(X,Z)) = .49E-27
Z = 2.21	X = .00	Re(W(X,Z)) = .63E-10	Re(U(X,Z)) = .19E-12
Z = 2.21	X = .10	Re(W(X,Z)) = .17E-10	Re(U(X,Z)) = .58E-10
Z = 2.21	X = .20	Re(W(X,Z)) = -.54E-10	Re(U(X,Z)) = .32E-10
Z = 2.21	X = .30	Re(W(X,Z)) = -.47E-10	Re(U(X,Z)) = -.41E-10
Z = 2.21	X = .40	Re(W(X,Z)) = .29E-10	Re(U(X,Z)) = -.54E-10
Z = 2.21	X = .50	Re(W(X,Z)) = .62E-10	Re(U(X,Z)) = .12E-10
Z = 1.52	X = .00	Re(W(X,Z)) = .30E-06	Re(U(X,Z)) = .16E-08
Z = 1.52	X = .10	Re(W(X,Z)) = .79E-07	Re(U(X,Z)) = .26E-06
Z = 1.52	X = .20	Re(W(X,Z)) = -.25E-06	Re(U(X,Z)) = .14E-06
Z = 1.52	X = .30	Re(W(X,Z)) = -.22E-06	Re(U(X,Z)) = -.18E-06
Z = 1.52	X = .40	Re(W(X,Z)) = .13E-06	Re(U(X,Z)) = -.24E-06
Z = 1.52	X = .50	Re(W(X,Z)) = .29E-06	Re(U(X,Z)) = .53E-07
Z = 1.11	X = .00	Re(W(X,Z)) = .31E-04	Re(U(X,Z)) = .32E-06
Z = 1.11	X = .10	Re(W(X,Z)) = .82E-05	Re(U(X,Z)) = .25E-04
Z = 1.11	X = .20	Re(W(X,Z)) = -.27E-04	Re(U(X,Z)) = .14E-04
Z = 1.11	X = .30	Re(W(X,Z)) = -.23E-04	Re(U(X,Z)) = -.18E-04
Z = 1.11	X = .40	Re(W(X,Z)) = .14E-04	Re(U(X,Z)) = -.23E-04
Z = 1.11	X = .50	Re(W(X,Z)) = .31E-04	Re(U(X,Z)) = .53E-05
Z = .82	X = .00	Re(W(X,Z)) = .53E-03	Re(U(X,Z)) = .14E-04
Z = .82	X = .10	Re(W(X,Z)) = .13E-03	Re(U(X,Z)) = .31E-03
Z = .82	X = .20	Re(W(X,Z)) = -.46E-03	Re(U(X,Z)) = .16E-03
Z = .82	X = .30	Re(W(X,Z)) = -.38E-03	Re(U(X,Z)) = -.23E-03
Z = .82	X = .40	Re(W(X,Z)) = .25E-03	Re(U(X,Z)) = -.28E-03
Z = .82	X = .50	Re(W(X,Z)) = .52E-03	Re(U(X,Z)) = .75E-04
Z = .60	X = .00	Re(W(X,Z)) = .22E-03	Re(U(X,Z)) = .36E-03
Z = .60	X = .10	Re(W(X,Z)) = -.26E-03	Re(U(X,Z)) = -.85E-03
Z = .60	X = .20	Re(W(X,Z)) = -.36E-03	Re(U(X,Z)) = -.82E-03
Z = .60	X = .30	Re(W(X,Z)) = .63E-04	Re(U(X,Z)) = .40E-03
Z = .60	X = .40	Re(W(X,Z)) = .40E-03	Re(U(X,Z)) = .10E-02
Z = .60	X = .50	Re(W(X,Z)) = .15E-03	Re(U(X,Z)) = .16E-03
Z = .57	X = .00	Re(W(X,Z)) = .13E-04	Re(U(X,Z)) = -.11E-15
Z = .57	X = .10	Re(W(X,Z)) = -.40E-03	Re(U(X,Z)) = .82E-15
Z = .57	X = .20	Re(W(X,Z)) = -.23E-03	Re(U(X,Z)) = .56E-15
Z = .57	X = .30	Re(W(X,Z)) = .27E-03	Re(U(X,Z)) = -.52E-15
Z = .57	X = .40	Re(W(X,Z)) = .38E-03	Re(U(X,Z)) = -.84E-15
Z = .57	X = .50	Re(W(X,Z)) = -.67E-04	Re(U(X,Z)) = .60E-16

For the mushy region:

Z = .57	X = .00	Re(W(X,Z)) = .13E-04	Re(U(X,Z)) = .26E-04
Z = .57	X = .10	Re(W(X,Z)) = -.40E-03	Re(U(X,Z)) = -.19E-04
Z = .57	X = .20	Re(W(X,Z)) = -.23E-03	Re(U(X,Z)) = -.36E-04
Z = .57	X = .30	Re(W(X,Z)) = .27E-03	Re(U(X,Z)) = -.93E-06
Z = .57	X = .40	Re(W(X,Z)) = .38E-03	Re(U(X,Z)) = .35E-04
Z = .57	X = .50	Re(W(X,Z)) = -.67E-04	Re(U(X,Z)) = .20E-04
Z = .42	X = .00	Re(W(X,Z)) = -.47E-04	Re(U(X,Z)) = .75E-03
Z = .42	X = .10	Re(W(X,Z)) = -.11E-02	Re(U(X,Z)) = .16E-03
Z = .42	X = .20	Re(W(X,Z)) = -.56E-03	Re(U(X,Z)) = -.66E-03
Z = .42	X = .30	Re(W(X,Z)) = .80E-03	Re(U(X,Z)) = -.52E-03
Z = .42	X = .40	Re(W(X,Z)) = .10E-02	Re(U(X,Z)) = .37E-03
Z = .42	X = .50	Re(W(X,Z)) = -.26E-03	Re(U(X,Z)) = .73E-03
Z = .29	X = .00	Re(W(X,Z)) = -.19E-03	Re(U(X,Z)) = .24E-02
Z = .29	X = .10	Re(W(X,Z)) = -.39E-02	Re(U(X,Z)) = .53E-03
Z = .29	X = .20	Re(W(X,Z)) = -.19E-02	Re(U(X,Z)) = -.21E-02
Z = .29	X = .30	Re(W(X,Z)) = .29E-02	Re(U(X,Z)) = -.17E-02
Z = .29	X = .40	Re(W(X,Z)) = .35E-02	Re(U(X,Z)) = .12E-02
Z = .29	X = .50	Re(W(X,Z)) = -.95E-03	Re(U(X,Z)) = .23E-02
Z = .18	X = .00	Re(W(X,Z)) = -.49E-03	Re(U(X,Z)) = .45E-02
Z = .18	X = .10	Re(W(X,Z)) = -.98E-02	Re(U(X,Z)) = .10E-02
Z = .18	X = .20	Re(W(X,Z)) = -.49E-02	Re(U(X,Z)) = -.40E-02
Z = .18	X = .30	Re(W(X,Z)) = .72E-02	Re(U(X,Z)) = -.32E-02
Z = .18	X = .40	Re(W(X,Z)) = .88E-02	Re(U(X,Z)) = .22E-02
Z = .18	X = .50	Re(W(X,Z)) = -.24E-02	Re(U(X,Z)) = .44E-02
Z = .09	X = .00	Re(W(X,Z)) = -.78E-03	Re(U(X,Z)) = .11E-02
Z = .09	X = .10	Re(W(X,Z)) = -.16E-01	Re(U(X,Z)) = .24E-03
Z = .09	X = .20	Re(W(X,Z)) = -.77E-02	Re(U(X,Z)) = -.96E-03
Z = .09	X = .30	Re(W(X,Z)) = .11E-01	Re(U(X,Z)) = -.76E-03
Z = .09	X = .40	Re(W(X,Z)) = .14E-01	Re(U(X,Z)) = .54E-03
Z = .09	X = .50	Re(W(X,Z)) = -.38E-02	Re(U(X,Z)) = .11E-02
Z = .00	X = .00	Re(W(X,Z)) = .00E+00	Re(U(X,Z)) = -.35E-01
Z = .00	X = .10	Re(W(X,Z)) = .00E+00	Re(U(X,Z)) = -.79E-02
Z = .00	X = .20	Re(W(X,Z)) = .00E+00	Re(U(X,Z)) = .31E-01
Z = .00	X = .30	Re(W(X,Z)) = .00E+00	Re(U(X,Z)) = .25E-01
Z = .00	X = .40	Re(W(X,Z)) = .00E+00	Re(U(X,Z)) = -.17E-01
Z = .00	X = .50	Re(W(X,Z)) = .00E+00	Re(U(X,Z)) = -.34E-01

Table 4

Am = .3 Al = .3E+05 Alpha = 2.21 Rm = 8.15 Wavelength = 2.84

For the liquid region:

Z = 5.20	X = .00	Re(W(X,Z)) = .73E-05	Re(U(X,Z)) = .35E-06
Z = 5.20	X = .60	Re(W(X,Z)) = .14E-05	Re(U(X,Z)) = .65E-05
Z = 5.20	X = 1.20	Re(W(X,Z)) = -.66E-05	Re(U(X,Z)) = .28E-05
Z = 5.20	X = 1.80	Re(W(X,Z)) = -.46E-05	Re(U(X,Z)) = -.51E-05
Z = 5.20	X = 2.40	Re(W(X,Z)) = .44E-05	Re(U(X,Z)) = -.53E-05
Z = 5.20	X = 3.00	Re(W(X,Z)) = .67E-05	Re(U(X,Z)) = .26E-05
Z = 2.21	X = .00	Re(W(X,Z)) = .17E-02	Re(U(X,Z)) = .30E-03
Z = 2.21	X = .60	Re(W(X,Z)) = .12E-03	Re(U(X,Z)) = .11E-02
Z = 2.21	X = 1.20	Re(W(X,Z)) = -.16E-02	Re(U(X,Z)) = .24E-03
Z = 2.21	X = 1.80	Re(W(X,Z)) = -.91E-03	Re(U(X,Z)) = -.10E-02
Z = 2.21	X = 2.40	Re(W(X,Z)) = .12E-02	Re(U(X,Z)) = -.73E-03
Z = 2.21	X = 3.00	Re(W(X,Z)) = .15E-02	Re(U(X,Z)) = .66E-03
Z = 1.52	X = .00	Re(W(X,Z)) = .35E-02	Re(U(X,Z)) = .15E-02
Z = 1.52	X = .60	Re(W(X,Z)) = -.56E-03	Re(U(X,Z)) = .87E-03
Z = 1.52	X = 1.20	Re(W(X,Z)) = -.37E-02	Re(U(X,Z)) = -.10E-02
Z = 1.52	X = 1.80	Re(W(X,Z)) = -.12E-02	Re(U(X,Z)) = -.14E-02
Z = 1.52	X = 2.40	Re(W(X,Z)) = .31E-02	Re(U(X,Z)) = .38E-03
Z = 1.52	X = 3.00	Re(W(X,Z)) = .28E-02	Re(U(X,Z)) = .16E-02
Z = 1.11	X = .00	Re(W(X,Z)) = .20E-02	Re(U(X,Z)) = .37E-02
Z = 1.11	X = .60	Re(W(X,Z)) = -.30E-02	Re(U(X,Z)) = -.43E-02
Z = 1.11	X = 1.20	Re(W(X,Z)) = -.34E-02	Re(U(X,Z)) = -.58E-02
Z = 1.11	X = 1.80	Re(W(X,Z)) = .14E-02	Re(U(X,Z)) = .15E-02
Z = 1.11	X = 2.40	Re(W(X,Z)) = .41E-02	Re(U(X,Z)) = .65E-02
Z = 1.11	X = 3.00	Re(W(X,Z)) = .62E-03	Re(U(X,Z)) = .16E-02
Z = .82	X = .00	Re(W(X,Z)) = -.52E-02	Re(U(X,Z)) = .71E-02
Z = .82	X = .60	Re(W(X,Z)) = -.80E-02	Re(U(X,Z)) = -.17E-01
Z = .82	X = 1.20	Re(W(X,Z)) = .13E-02	Re(U(X,Z)) = -.15E-01
Z = .82	X = 1.80	Re(W(X,Z)) = .86E-02	Re(U(X,Z)) = .95E-02
Z = .82	X = 2.40	Re(W(X,Z)) = .28E-02	Re(U(X,Z)) = .20E-01
Z = .82	X = 3.00	Re(W(X,Z)) = -.72E-02	Re(U(X,Z)) = .10E-03
Z = .60	X = .00	Re(W(X,Z)) = -.20E-01	Re(U(X,Z)) = .63E-02
Z = .60	X = .60	Re(W(X,Z)) = -.16E-01	Re(U(X,Z)) = -.30E-01
Z = .60	X = 1.20	Re(W(X,Z)) = .12E-01	Re(U(X,Z)) = -.21E-01
Z = .60	X = 1.80	Re(W(X,Z)) = .21E-01	Re(U(X,Z)) = .20E-01
Z = .60	X = 2.40	Re(W(X,Z)) = -.17E-02	Re(U(X,Z)) = .31E-01
Z = .60	X = 3.00	Re(W(X,Z)) = -.22E-01	Re(U(X,Z)) = -.52E-02
Z = .57	X = .00	Re(W(X,Z)) = -.21E-01	Re(U(X,Z)) = .36E-14
Z = .57	X = .60	Re(W(X,Z)) = -.16E-01	Re(U(X,Z)) = -.86E-15
Z = .57	X = 1.20	Re(W(X,Z)) = .13E-01	Re(U(X,Z)) = -.40E-14
Z = .57	X = 1.80	Re(W(X,Z)) = .22E-01	Re(U(X,Z)) = -.11E-14
Z = .57	X = 2.40	Re(W(X,Z)) = -.22E-02	Re(U(X,Z)) = .35E-14
Z = .57	X = 3.00	Re(W(X,Z)) = -.23E-01	Re(U(X,Z)) = .27E-14

For the mushy region:

Z = .57	X = .00	Re(W(X,Z)) = -.21E-01	Re(U(X,Z)) = .66E-04
Z = .57	X = .60	Re(W(X,Z)) = -.16E-01	Re(U(X,Z)) = -.13E-02
Z = .57	X = 1.20	Re(W(X,Z)) = .13E-01	Re(U(X,Z)) = -.68E-03
Z = .57	X = 1.80	Re(W(X,Z)) = .22E-01	Re(U(X,Z)) = .93E-03
Z = .57	X = 2.40	Re(W(X,Z)) = -.22E-02	Re(U(X,Z)) = .11E-02
Z = .57	X = 3.00	Re(W(X,Z)) = -.23E-01	Re(U(X,Z)) = -.38E-03
Z = .42	X = .00	Re(W(X,Z)) = -.20E-01	Re(U(X,Z)) = -.27E-02
Z = .42	X = .60	Re(W(X,Z)) = -.16E-01	Re(U(X,Z)) = .30E-02
Z = .42	X = 1.20	Re(W(X,Z)) = .13E-01	Re(U(X,Z)) = .42E-02
Z = .42	X = 1.80	Re(W(X,Z)) = .22E-01	Re(U(X,Z)) = -.99E-03
Z = .42	X = 2.40	Re(W(X,Z)) = -.23E-02	Re(U(X,Z)) = -.46E-02
Z = .42	X = 3.00	Re(W(X,Z)) = -.23E-01	Re(U(X,Z)) = -.13E-02
Z = .29	X = .00	Re(W(X,Z)) = -.18E-01	Re(U(X,Z)) = -.62E-02
Z = .29	X = .60	Re(W(X,Z)) = -.13E-01	Re(U(X,Z)) = .90E-02
Z = .29	X = 1.20	Re(W(X,Z)) = .11E-01	Re(U(X,Z)) = .11E-01
Z = .29	X = 1.80	Re(W(X,Z)) = .19E-01	Re(U(X,Z)) = -.39E-02
Z = .29	X = 2.40	Re(W(X,Z)) = -.22E-02	Re(U(X,Z)) = -.13E-01
Z = .29	X = 3.00	Re(W(X,Z)) = -.20E-01	Re(U(X,Z)) = -.22E-02
Z = .18	X = .00	Re(W(X,Z)) = -.14E-01	Re(U(X,Z)) = -.10E-01
Z = .18	X = .60	Re(W(X,Z)) = -.10E-01	Re(U(X,Z)) = .16E-01
Z = .18	X = 1.20	Re(W(X,Z)) = .88E-02	Re(U(X,Z)) = .18E-01
Z = .18	X = 1.80	Re(W(X,Z)) = .14E-01	Re(U(X,Z)) = -.72E-02
Z = .18	X = 2.40	Re(W(X,Z)) = -.18E-02	Re(U(X,Z)) = -.21E-01
Z = .18	X = 3.00	Re(W(X,Z)) = -.15E-01	Re(U(X,Z)) = -.31E-02
Z = .09	X = .00	Re(W(X,Z)) = -.76E-02	Re(U(X,Z)) = -.14E-01
Z = .09	X = .60	Re(W(X,Z)) = -.56E-02	Re(U(X,Z)) = .24E-01
Z = .09	X = 1.20	Re(W(X,Z)) = .49E-02	Re(U(X,Z)) = .26E-01
Z = .09	X = 1.80	Re(W(X,Z)) = .80E-02	Re(U(X,Z)) = -.11E-01
Z = .09	X = 2.40	Re(W(X,Z)) = -.11E-02	Re(U(X,Z)) = -.31E-01
Z = .09	X = 3.00	Re(W(X,Z)) = -.85E-02	Re(U(X,Z)) = -.40E-02
Z = .00	X = .00	Re(W(X,Z)) = .00E+00	Re(U(X,Z)) = -.19E-01
Z = .00	X = .60	Re(W(X,Z)) = .00E+00	Re(U(X,Z)) = .32E-01
Z = .00	X = 1.20	Re(W(X,Z)) = .00E+00	Re(U(X,Z)) = .35E-01
Z = .00	X = 1.80	Re(W(X,Z)) = .00E+00	Re(U(X,Z)) = -.15E-01
Z = .00	X = 2.40	Re(W(X,Z)) = .00E+00	Re(U(X,Z)) = -.42E-01
Z = .00	X = 3.00	Re(W(X,Z)) = .00E+00	Re(U(X,Z)) = -.49E-02

Table 5

Am = .3 Al = .3E+05 Alpha = 13.55 Rm = 8.62 Wavelength = .46

For the liquid region:

Z = 5.20	X = .00	Re(W(X,Z)) = .16E-27	Re(U(X,Z)) = .39E-30
Z = 5.20	X = .10	Re(W(X,Z)) = .34E-28	Re(U(X,Z)) = .16E-27
Z = 5.20	X = .20	Re(W(X,Z)) = -.15E-27	Re(U(X,Z)) = .67E-28
Z = 5.20	X = .30	Re(W(X,Z)) = -.98E-28	Re(U(X,Z)) = -.13E-27
Z = 5.20	X = .40	Re(W(X,Z)) = .11E-27	Re(U(X,Z)) = -.12E-27
Z = 5.20	X = .50	Re(W(X,Z)) = .14E-27	Re(U(X,Z)) = .76E-28
Z = 2.21	X = .00	Re(W(X,Z)) = .24E-10	Re(U(X,Z)) = .18E-12
Z = 2.21	X = .10	Re(W(X,Z)) = .50E-11	Re(U(X,Z)) = .22E-10
Z = 2.21	X = .20	Re(W(X,Z)) = -.22E-10	Re(U(X,Z)) = .94E-11
Z = 2.21	X = .30	Re(W(X,Z)) = -.14E-10	Re(U(X,Z)) = -.18E-10
Z = 2.21	X = .40	Re(W(X,Z)) = .16E-10	Re(U(X,Z)) = -.17E-10
Z = 2.21	X = .50	Re(W(X,Z)) = .21E-10	Re(U(X,Z)) = .11E-10
Z = 1.52	X = .00	Re(W(X,Z)) = .17E-06	Re(U(X,Z)) = .23E-08
Z = 1.52	X = .10	Re(W(X,Z)) = .34E-07	Re(U(X,Z)) = .15E-06
Z = 1.52	X = .20	Re(W(X,Z)) = -.16E-06	Re(U(X,Z)) = .63E-07
Z = 1.52	X = .30	Re(W(X,Z)) = -.10E-06	Re(U(X,Z)) = -.13E-06
Z = 1.52	X = .40	Re(W(X,Z)) = .11E-06	Re(U(X,Z)) = -.12E-06
Z = 1.52	X = .50	Re(W(X,Z)) = .15E-06	Re(U(X,Z)) = .76E-07
Z = 1.11	X = .00	Re(W(X,Z)) = .23E-04	Re(U(X,Z)) = .58E-06
Z = 1.11	X = .10	Re(W(X,Z)) = .43E-05	Re(U(X,Z)) = .19E-04
Z = 1.11	X = .20	Re(W(X,Z)) = -.21E-04	Re(U(X,Z)) = .76E-05
Z = 1.11	X = .30	Re(W(X,Z)) = -.13E-04	Re(U(X,Z)) = -.16E-04
Z = 1.11	X = .40	Re(W(X,Z)) = .15E-04	Re(U(X,Z)) = -.14E-04
Z = 1.11	X = .50	Re(W(X,Z)) = .20E-04	Re(U(X,Z)) = .97E-05
Z = .82	X = .00	Re(W(X,Z)) = .45E-03	Re(U(X,Z)) = .29E-04
Z = .82	X = .10	Re(W(X,Z)) = .69E-04	Re(U(X,Z)) = .28E-03
Z = .82	X = .20	Re(W(X,Z)) = -.42E-03	Re(U(X,Z)) = .90E-04
Z = .82	X = .30	Re(W(X,Z)) = -.25E-03	Re(U(X,Z)) = -.24E-03
Z = .82	X = .40	Re(W(X,Z)) = .32E-03	Re(U(X,Z)) = -.19E-03
Z = .82	X = .50	Re(W(X,Z)) = .39E-03	Re(U(X,Z)) = .16E-03
Z = .60	X = .00	Re(W(X,Z)) = .96E-04	Re(U(X,Z)) = .90E-03
Z = .60	X = .10	Re(W(X,Z)) = -.80E-03	Re(U(X,Z)) = -.79E-03
Z = .60	X = .20	Re(W(X,Z)) = -.44E-03	Re(U(X,Z)) = -.12E-02
Z = .60	X = .30	Re(W(X,Z)) = .61E-03	Re(U(X,Z)) = .26E-03
Z = .60	X = .40	Re(W(X,Z)) = .70E-03	Re(U(X,Z)) = .13E-02
Z = .60	X = .50	Re(W(X,Z)) = -.31E-03	Re(U(X,Z)) = .32E-03
Z = .57	X = .00	Re(W(X,Z)) = -.13E-03	Re(U(X,Z)) = .22E-15
Z = .57	X = .10	Re(W(X,Z)) = -.11E-02	Re(U(X,Z)) = .92E-15
Z = .57	X = .20	Re(W(X,Z)) = -.33E-03	Re(U(X,Z)) = .17E-15
Z = .57	X = .30	Re(W(X,Z)) = .93E-03	Re(U(X,Z)) = -.84E-15
Z = .57	X = .40	Re(W(X,Z)) = .73E-03	Re(U(X,Z)) = -.53E-15
Z = .57	X = .50	Re(W(X,Z)) = -.62E-03	Re(U(X,Z)) = .62E-15

For the mushy region:

Z = .57	X = .00	Re(W(X,Z)) = -.13E-03	Re(U(X,Z)) = .64E-04
Z = .57	X = .10	Re(W(X,Z)) = -.11E-02	Re(U(X,Z)) = -.18E-04
Z = .57	X = .20	Re(W(X,Z)) = -.33E-03	Re(U(X,Z)) = -.72E-04
Z = .57	X = .30	Re(W(X,Z)) = .93E-03	Re(U(X,Z)) = -.13E-04
Z = .57	X = .40	Re(W(X,Z)) = .73E-03	Re(U(X,Z)) = .67E-04
Z = .57	X = .50	Re(W(X,Z)) = -.62E-03	Re(U(X,Z)) = .41E-04
Z = .42	X = .00	Re(W(X,Z)) = -.47E-03	Re(U(X,Z)) = .21E-02
Z = .42	X = .10	Re(W(X,Z)) = -.31E-02	Re(U(X,Z)) = .13E-03
Z = .42	X = .20	Re(W(X,Z)) = -.88E-03	Re(U(X,Z)) = -.20E-02
Z = .42	X = .30	Re(W(X,Z)) = .28E-02	Re(U(X,Z)) = -.10E-02
Z = .42	X = .40	Re(W(X,Z)) = .21E-02	Re(U(X,Z)) = .16E-02
Z = .42	X = .50	Re(W(X,Z)) = -.19E-02	Re(U(X,Z)) = .17E-02
Z = .29	X = .00	Re(W(X,Z)) = -.18E-02	Re(U(X,Z)) = .71E-02
Z = .29	X = .10	Re(W(X,Z)) = -.12E-01	Re(U(X,Z)) = .45E-03
Z = .29	X = .20	Re(W(X,Z)) = -.33E-02	Re(U(X,Z)) = -.69E-02
Z = .29	X = .30	Re(W(X,Z)) = .11E-01	Re(U(X,Z)) = -.34E-02
Z = .29	X = .40	Re(W(X,Z)) = .79E-02	Re(U(X,Z)) = .55E-02
Z = .29	X = .50	Re(W(X,Z)) = -.72E-02	Re(U(X,Z)) = .58E-02
Z = .18	X = .00	Re(W(X,Z)) = -.49E-02	Re(U(X,Z)) = .15E-01
Z = .18	X = .10	Re(W(X,Z)) = -.32E-01	Re(U(X,Z)) = .91E-03
Z = .18	X = .20	Re(W(X,Z)) = -.88E-02	Re(U(X,Z)) = -.14E-01
Z = .18	X = .30	Re(W(X,Z)) = .28E-01	Re(U(X,Z)) = -.71E-02
Z = .18	X = .40	Re(W(X,Z)) = .21E-01	Re(U(X,Z)) = .11E-01
Z = .18	X = .50	Re(W(X,Z)) = -.19E-01	Re(U(X,Z)) = .12E-01
Z = .09	X = .00	Re(W(X,Z)) = -.83E-02	Re(U(X,Z)) = .53E-02
Z = .09	X = .10	Re(W(X,Z)) = -.54E-01	Re(U(X,Z)) = .30E-03
Z = .09	X = .20	Re(W(X,Z)) = -.15E-01	Re(U(X,Z)) = -.52E-02
Z = .09	X = .30	Re(W(X,Z)) = .48E-01	Re(U(X,Z)) = -.25E-02
Z = .09	X = .40	Re(W(X,Z)) = .35E-01	Re(U(X,Z)) = .41E-02
Z = .09	X = .50	Re(W(X,Z)) = -.33E-01	Re(U(X,Z)) = .43E-02
Z = .00	X = .00	Re(W(X,Z)) = .00E+00	Re(U(X,Z)) = -.12E+00
Z = .00	X = .10	Re(W(X,Z)) = -.11E-12	Re(U(X,Z)) = -.72E-02
Z = .00	X = .20	Re(W(X,Z)) = -.48E-13	Re(U(X,Z)) = .11E+00
Z = .00	X = .30	Re(W(X,Z)) = .91E-13	Re(U(X,Z)) = .56E-01
Z = .00	X = .40	Re(W(X,Z)) = .86E-13	Re(U(X,Z)) = -.90E-01
Z = .00	X = .50	Re(W(X,Z)) = -.54E-13	Re(U(X,Z)) = -.95E-01

Table 6

Am = .6 Al = .6E+05 Alpha = 2.26 Rm = 9.40 Wavelength = 2.78

For the liquid region:

Z = 5.20	X = .00	Re(W(X,Z)) = .57E-05	Re(U(X,Z)) = .18E-06
Z = 5.20	X = .60	Re(W(X,Z)) = .10E-05	Re(U(X,Z)) = .51E-05
Z = 5.20	X = 1.20	Re(W(X,Z)) = -.53E-05	Re(U(X,Z)) = .20E-05
Z = 5.20	X = 1.80	Re(W(X,Z)) = -.33E-05	Re(U(X,Z)) = -.42E-05
Z = 5.20	X = 2.40	Re(W(X,Z)) = .39E-05	Re(U(X,Z)) = -.38E-05
Z = 5.20	X = 3.00	Re(W(X,Z)) = .49E-05	Re(U(X,Z)) = .26E-05
Z = 2.21	X = .00	Re(W(X,Z)) = .15E-02	Re(U(X,Z)) = .18E-03
Z = 2.21	X = .60	Re(W(X,Z)) = .14E-03	Re(U(X,Z)) = .94E-03
Z = 2.21	X = 1.20	Re(W(X,Z)) = -.14E-02	Re(U(X,Z)) = .22E-03
Z = 2.21	X = 1.80	Re(W(X,Z)) = -.74E-03	Re(U(X,Z)) = -.85E-03
Z = 2.21	X = 2.40	Re(W(X,Z)) = .11E-02	Re(U(X,Z)) = -.58E-03
Z = 2.21	X = 3.00	Re(W(X,Z)) = .12E-02	Re(U(X,Z)) = .60E-03
Z = 1.52	X = .00	Re(W(X,Z)) = .29E-02	Re(U(X,Z)) = .90E-03
Z = 1.52	X = .60	Re(W(X,Z)) = -.25E-03	Re(U(X,Z)) = .32E-03
Z = 1.52	X = 1.20	Re(W(X,Z)) = -.30E-02	Re(U(X,Z)) = -.76E-03
Z = 1.52	X = 1.80	Re(W(X,Z)) = -.10E-02	Re(U(X,Z)) = -.64E-03
Z = 1.52	X = 2.40	Re(W(X,Z)) = .25E-02	Re(U(X,Z)) = .49E-03
Z = 1.52	X = 3.00	Re(W(X,Z)) = .21E-02	Re(U(X,Z)) = .85E-03
Z = 1.11	X = .00	Re(W(X,Z)) = .81E-03	Re(U(X,Z)) = .23E-02
Z = 1.11	X = .60	Re(W(X,Z)) = -.20E-02	Re(U(X,Z)) = -.56E-02
Z = 1.11	X = 1.20	Re(W(X,Z)) = -.17E-02	Re(U(X,Z)) = -.47E-02
Z = 1.11	X = 1.80	Re(W(X,Z)) = .13E-02	Re(U(X,Z)) = .36E-02
Z = 1.11	X = 2.40	Re(W(X,Z)) = .22E-02	Re(U(X,Z)) = .62E-02
Z = 1.11	X = 3.00	Re(W(X,Z)) = -.36E-03	Re(U(X,Z)) = -.93E-03
Z = .82	X = .00	Re(W(X,Z)) = -.73E-02	Re(U(X,Z)) = .45E-02
Z = .82	X = .60	Re(W(X,Z)) = -.58E-02	Re(U(X,Z)) = -.19E-01
Z = .82	X = 1.20	Re(W(X,Z)) = .48E-02	Re(U(X,Z)) = -.13E-01
Z = .82	X = 1.80	Re(W(X,Z)) = .79E-02	Re(U(X,Z)) = .14E-01
Z = .82	X = 2.40	Re(W(X,Z)) = -.14E-02	Re(U(X,Z)) = .19E-01
Z = .82	X = 3.00	Re(W(X,Z)) = -.85E-02	Re(U(X,Z)) = -.60E-02
Z = .60	X = .00	Re(W(X,Z)) = -.23E-01	Re(U(X,Z)) = -.22E-02
Z = .60	X = .60	Re(W(X,Z)) = -.11E-01	Re(U(X,Z)) = -.36E-01
Z = .60	X = 1.20	Re(W(X,Z)) = .18E-01	Re(U(X,Z)) = -.13E-01
Z = .60	X = 1.80	Re(W(X,Z)) = .19E-01	Re(U(X,Z)) = .31E-01
Z = .60	X = 2.40	Re(W(X,Z)) = -.10E-01	Re(U(X,Z)) = .26E-01
Z = .60	X = 3.00	Re(W(X,Z)) = -.24E-01	Re(U(X,Z)) = -.19E-01
Z = .57	X = .00	Re(W(X,Z)) = -.25E-01	Re(U(X,Z)) = -.36E-14
Z = .57	X = .60	Re(W(X,Z)) = -.11E-01	Re(U(X,Z)) = .98E-15
Z = .57	X = 1.20	Re(W(X,Z)) = .20E-01	Re(U(X,Z)) = .40E-14
Z = .57	X = 1.80	Re(W(X,Z)) = .20E-01	Re(U(X,Z)) = .71E-15
Z = .57	X = 2.40	Re(W(X,Z)) = -.11E-01	Re(U(X,Z)) = -.37E-14
Z = .57	X = 3.00	Re(W(X,Z)) = -.25E-01	Re(U(X,Z)) = -.23E-14

For the mushy region:

Z = .57	X = .00	Re(W(X,Z)) = -.25E-01	Re(U(X,Z)) = -.57E-03
Z = .57	X = .60	Re(W(X,Z)) = -.11E-01	Re(U(X,Z)) = -.16E-02
Z = .57	X = 1.20	Re(W(X,Z)) = .20E-01	Re(U(X,Z)) = -.12E-03
Z = .57	X = 1.80	Re(W(X,Z)) = .20E-01	Re(U(X,Z)) = .16E-02
Z = .57	X = 2.40	Re(W(X,Z)) = -.11E-01	Re(U(X,Z)) = .79E-03
Z = .57	X = 3.00	Re(W(X,Z)) = -.25E-01	Re(U(X,Z)) = -.12E-02
Z = .42	X = .00	Re(W(X,Z)) = -.24E-01	Re(U(X,Z)) = -.20E-02
Z = .42	X = .60	Re(W(X,Z)) = -.11E-01	Re(U(X,Z)) = .42E-02
Z = .42	X = 1.20	Re(W(X,Z)) = .20E-01	Re(U(X,Z)) = .38E-02
Z = .42	X = 1.80	Re(W(X,Z)) = .19E-01	Re(U(X,Z)) = -.26E-02
Z = .42	X = 2.40	Re(W(X,Z)) = -.11E-01	Re(U(X,Z)) = -.49E-02
Z = .42	X = 3.00	Re(W(X,Z)) = -.24E-01	Re(U(X,Z)) = .49E-03
Z = .29	X = .00	Re(W(X,Z)) = -.21E-01	Re(U(X,Z)) = -.37E-02
Z = .29	X = .60	Re(W(X,Z)) = -.93E-02	Re(U(X,Z)) = .12E-01
Z = .29	X = 1.20	Re(W(X,Z)) = .17E-01	Re(U(X,Z)) = .88E-02
Z = .29	X = 1.80	Re(W(X,Z)) = .17E-01	Re(U(X,Z)) = -.82E-02
Z = .29	X = 2.40	Re(W(X,Z)) = -.10E-01	Re(U(X,Z)) = -.12E-01
Z = .29	X = 3.00	Re(W(X,Z)) = -.21E-01	Re(U(X,Z)) = .30E-02
Z = .18	X = .00	Re(W(X,Z)) = -.16E-01	Re(U(X,Z)) = -.54E-02
Z = .18	X = .60	Re(W(X,Z)) = -.69E-02	Re(U(X,Z)) = .20E-01
Z = .18	X = 1.20	Re(W(X,Z)) = .13E-01	Re(U(X,Z)) = .14E-01
Z = .18	X = 1.80	Re(W(X,Z)) = .12E-01	Re(U(X,Z)) = -.14E-01
Z = .18	X = 2.40	Re(W(X,Z)) = -.77E-02	Re(U(X,Z)) = -.20E-01
Z = .18	X = 3.00	Re(W(X,Z)) = -.16E-01	Re(U(X,Z)) = .58E-02
Z = .09	X = .00	Re(W(X,Z)) = -.88E-02	Re(U(X,Z)) = -.71E-02
Z = .09	X = .60	Re(W(X,Z)) = -.37E-02	Re(U(X,Z)) = .29E-01
Z = .09	X = 1.20	Re(W(X,Z)) = .72E-02	Re(U(X,Z)) = .20E-01
Z = .09	X = 1.80	Re(W(X,Z)) = .68E-02	Re(U(X,Z)) = -.21E-01
Z = .09	X = 2.40	Re(W(X,Z)) = -.43E-02	Re(U(X,Z)) = -.29E-01
Z = .09	X = 3.00	Re(W(X,Z)) = -.86E-02	Re(U(X,Z)) = .89E-02
Z = .00	X = .00	Re(W(X,Z)) = .18E-14	Re(U(X,Z)) = -.89E-02
Z = .00	X = .60	Re(W(X,Z)) = .12E-14	Re(U(X,Z)) = .39E-01
Z = .00	X = 1.20	Re(W(X,Z)) = -.12E-14	Re(U(X,Z)) = .26E-01
Z = .00	X = 1.80	Re(W(X,Z)) = -.18E-14	Re(U(X,Z)) = -.28E-01
Z = .00	X = 2.40	Re(W(X,Z)) = .49E-15	Re(U(X,Z)) = -.38E-01
Z = .00	X = 3.00	Re(W(X,Z)) = .20E-14	Re(U(X,Z)) = .12E-01

Table 7

Am = .6 Al = .6E+05 Alpha = 15.40 Rm = 10.25 Wavelength = .41

For the liquid region:

Z = 5.20	X = .00	Re(W(X,Z)) = .32E-31	Re(U(X,Z)) = .87E-34
Z = 5.20	X = .10	Re(W(X,Z)) = .91E-33	Re(U(X,Z)) = .32E-31
Z = 5.20	X = .20	Re(W(X,Z)) = -.32E-31	Re(U(X,Z)) = .19E-32
Z = 5.20	X = .30	Re(W(X,Z)) = -.29E-32	Re(U(X,Z)) = -.32E-31
Z = 5.20	X = .40	Re(W(X,Z)) = .32E-31	Re(U(X,Z)) = -.38E-32
Z = 2.21	X = .00	Re(W(X,Z)) = .12E-11	Re(U(X,Z)) = .10E-13
Z = 2.21	X = .10	Re(W(X,Z)) = .27E-13	Re(U(X,Z)) = .12E-11
Z = 2.21	X = .20	Re(W(X,Z)) = -.12E-11	Re(U(X,Z)) = .61E-13
Z = 2.21	X = .30	Re(W(X,Z)) = -.10E-12	Re(U(X,Z)) = -.12E-11
Z = 2.21	X = .40	Re(W(X,Z)) = .12E-11	Re(U(X,Z)) = -.13E-12
Z = 1.52	X = .00	Re(W(X,Z)) = .31E-07	Re(U(X,Z)) = .48E-09
Z = 1.52	X = .10	Re(W(X,Z)) = .47E-09	Re(U(X,Z)) = .29E-07
Z = 1.52	X = .20	Re(W(X,Z)) = -.31E-07	Re(U(X,Z)) = .13E-08
Z = 1.52	X = .30	Re(W(X,Z)) = -.24E-08	Re(U(X,Z)) = -.28E-07
Z = 1.52	X = .40	Re(W(X,Z)) = .31E-07	Re(U(X,Z)) = -.30E-08
Z = 1.11	X = .00	Re(W(X,Z)) = .87E-05	Re(U(X,Z)) = .25E-06
Z = 1.11	X = .10	Re(W(X,Z)) = .16E-07	Re(U(X,Z)) = .75E-05
Z = 1.11	X = .20	Re(W(X,Z)) = -.87E-05	Re(U(X,Z)) = .21E-06
Z = 1.11	X = .30	Re(W(X,Z)) = -.55E-06	Re(U(X,Z)) = -.75E-05
Z = 1.11	X = .40	Re(W(X,Z)) = .87E-05	Re(U(X,Z)) = -.67E-06
Z = .82	X = .00	Re(W(X,Z)) = .29E-03	Re(U(X,Z)) = .22E-04
Z = .82	X = .10	Re(W(X,Z)) = -.13E-04	Re(U(X,Z)) = .19E-03
Z = .82	X = .20	Re(W(X,Z)) = -.29E-03	Re(U(X,Z)) = -.10E-04
Z = .82	X = .30	Re(W(X,Z)) = -.51E-05	Re(U(X,Z)) = -.19E-03
Z = .82	X = .40	Re(W(X,Z)) = .29E-03	Re(U(X,Z)) = -.13E-05
Z = .60	X = .00	Re(W(X,Z)) = -.53E-04	Re(U(X,Z)) = .11E-02
Z = .60	X = .10	Re(W(X,Z)) = -.11E-02	Re(U(X,Z)) = -.85E-03
Z = .60	X = .20	Re(W(X,Z)) = -.12E-04	Re(U(X,Z)) = -.12E-02
Z = .60	X = .30	Re(W(X,Z)) = .11E-02	Re(U(X,Z)) = .78E-03
Z = .60	X = .40	Re(W(X,Z)) = .77E-04	Re(U(X,Z)) = .12E-02
Z = .57	X = .00	Re(W(X,Z)) = -.29E-03	Re(U(X,Z)) = -.13E-14
Z = .57	X = .10	Re(W(X,Z)) = -.14E-02	Re(U(X,Z)) = -.36E-14
Z = .57	X = .20	Re(W(X,Z)) = .20E-03	Re(U(X,Z)) = .11E-14
Z = .57	X = .30	Re(W(X,Z)) = .14E-02	Re(U(X,Z)) = .37E-14
Z = .57	X = .40	Re(W(X,Z)) = -.11E-03	Re(U(X,Z)) = -.89E-15

For the mushy region:

Z = .57	X = .00	Re(W(X,Z)) = -.29E-03	Re(U(X,Z)) = .74E-04
Z = .57	X = .10	Re(W(X,Z)) = -.14E-02	Re(U(X,Z)) = -.29E-04
Z = .57	X = .20	Re(W(X,Z)) = .20E-03	Re(U(X,Z)) = -.76E-04
Z = .57	X = .30	Re(W(X,Z)) = .14E-02	Re(U(X,Z)) = .25E-04
Z = .57	X = .40	Re(W(X,Z)) = -.11E-03	Re(U(X,Z)) = .78E-04
Z = .42	X = .00	Re(W(X,Z)) = -.11E-02	Re(U(X,Z)) = .35E-02
Z = .42	X = .10	Re(W(X,Z)) = -.51E-02	Re(U(X,Z)) = -.69E-03
Z = .42	X = .20	Re(W(X,Z)) = .82E-03	Re(U(X,Z)) = -.35E-02
Z = .42	X = .30	Re(W(X,Z)) = .51E-02	Re(U(X,Z)) = .47E-03
Z = .42	X = .40	Re(W(X,Z)) = -.50E-03	Re(U(X,Z)) = .36E-02
Z = .29	X = .00	Re(W(X,Z)) = -.56E-02	Re(U(X,Z)) = .15E-01
Z = .29	X = .10	Re(W(X,Z)) = -.25E-01	Re(U(X,Z)) = -.30E-02
Z = .29	X = .20	Re(W(X,Z)) = .40E-02	Re(U(X,Z)) = -.15E-01
Z = .29	X = .30	Re(W(X,Z)) = .25E-01	Re(U(X,Z)) = .21E-02
Z = .29	X = .40	Re(W(X,Z)) = -.25E-02	Re(U(X,Z)) = .15E-01
Z = .18	X = .00	Re(W(X,Z)) = -.18E-01	Re(U(X,Z)) = .40E-01
Z = .18	X = .10	Re(W(X,Z)) = -.79E-01	Re(U(X,Z)) = -.79E-02
Z = .18	X = .20	Re(W(X,Z)) = .13E-01	Re(U(X,Z)) = -.40E-01
Z = .18	X = .30	Re(W(X,Z)) = .80E-01	Re(U(X,Z)) = .55E-02
Z = .18	X = .40	Re(W(X,Z)) = -.82E-02	Re(U(X,Z)) = .40E-01
Z = .09	X = .00	Re(W(X,Z)) = -.36E-01	Re(U(X,Z)) = .29E-01
Z = .09	X = .10	Re(W(X,Z)) = -.16E+00	Re(U(X,Z)) = -.58E-02
Z = .09	X = .20	Re(W(X,Z)) = .27E-01	Re(U(X,Z)) = -.29E-01
Z = .09	X = .30	Re(W(X,Z)) = .16E+00	Re(U(X,Z)) = .41E-02
Z = .09	X = .40	Re(W(X,Z)) = -.17E-01	Re(U(X,Z)) = .29E-01
Z = .00	X = .00	Re(W(X,Z)) = .15E-10	Re(U(X,Z)) = -.36E+00
Z = .00	X = .10	Re(W(X,Z)) = .14E-11	Re(U(X,Z)) = .72E-01
Z = .00	X = .20	Re(W(X,Z)) = -.14E-10	Re(U(X,Z)) = .36E+00
Z = .00	X = .30	Re(W(X,Z)) = -.22E-11	Re(U(X,Z)) = -.49E-01
Z = .00	X = .40	Re(W(X,Z)) = .14E-10	Re(U(X,Z)) = -.36E+00

Table 8

List of Recent TAM Reports

No.	Authors	Title	Date
717	Nitzsche, V. R., and K. J. Hsia	Modelling of dislocation mobility controlled brittle-to-ductile transition	July 1993
718	Hsia, K. J., and A. S. Argon	Experimental study of the mechanisms of brittle-to-ductile transition of cleavage fracture in silicon single crystals	July 1993
719	Cherukuri, H. P., and T. G. Shawki	An energy-based localization theory: Part II—Effects of the diffusion, inertia and dissipation numbers	Aug. 1993
720	Aref, H., and S. W. Jones	Chaotic motion of a solid through ideal fluid	Aug. 1993
721	Stewart, D. S.	Lectures on detonation physics: Introduction to the theory of detonation shock dynamics	Aug. 1993
722	Lawrence, C. J., and R. Mei	Long-time behavior of the drag on a body in impulsive motion	Sept. 1993
723	Mei, R., J. F. Klausner, and C. J. Lawrence	A note on the history force on a spherical bubble at finite Reynolds number	Sept. 1993
724	Qi, Q., R. E. Johnson, and J. G. Harris	A re-examination of the boundary layer attenuation and acoustic streaming accompanying plane wave propagation in a circular tube	Sept. 1993
725	Turner, J. A., and R. L. Weaver	Radiative transfer of ultrasound	Sept. 1993
726	Yogeswaren, E. K., and J. G. Harris	A model of a confocal ultrasonic inspection system for interfaces	Sept. 1993
727	Yao, J., and D. S. Stewart	On the normal detonation shock velocity–curvature relationship for materials with large activation energy	Sept. 1993
728	Qi, Q.	Attenuated leaky Rayleigh waves	Oct. 1993
729	Sofronis, P., and H. K. Birnbaum	Mechanics of hydrogen–dislocation–impurity interactions: Part I—Increasing shear modulus	Oct. 1993
730	Hsia, K. J., Z. Suo, and W. Yang	Cleavage due to dislocation confinement in layered materials	Oct. 1993
731	Acharya, A., and T. G. Shawki	A second-deformation-gradient theory of plasticity	Oct. 1993
732	Michaleris, P., D. A. Tortorelli, and C. A. Vidal	Tangent operators and design sensitivity formulations for transient nonlinear coupled problems with applications to elasto-plasticity	Nov. 1993
733	Michaleris, P., D. A. Tortorelli, and C. A. Vidal	Analysis and optimization of weakly coupled thermo-elasto-plastic systems with applications to weldment design	Nov. 1993
734	Ford, D. K., and D. S. Stewart	Probabilistic modeling of propellant beds exposed to strong stimulus	Nov. 1993
735	Mei, R., R. J. Adrian, and T. J. Hanratty	Particle dispersion in isotropic turbulence under the influence of non-Stokesian drag and gravitational settling	Nov. 1993
736	Dey, N., D. F. Socie, and K. J. Hsia	Static and cyclic fatigue failure at high temperature in ceramics containing grain boundary viscous phase: Part I—Experiments	Nov. 1993
737	Dey, N., D. F. Socie, and K. J. Hsia	Static and cyclic fatigue failure at high temperature in ceramics containing grain boundary viscous phase: Part II—Modelling	Nov. 1993
738	Turner, J. A., and R. L. Weaver	Radiative transfer and multiple scattering of diffuse ultrasound in polycrystalline media	Nov. 1993
739	Qi, Q., and R. E. Johnson	Resin flows through a porous fiber collection in pultrusion processing	Dec. 1993
740	Weaver, R. L., W. Sachse, and K. Y. Kim	Transient elastic waves in a transversely isotropic plate	Dec. 1993
741	Zhang, Y., and R. L. Weaver	Scattering from a thin random fluid layer	Dec. 1993
742	Weaver, R. L., and W. Sachse	Diffusion of ultrasound in a glass bead slurry	Dec. 1993

List of Recent TAM Reports (cont'd)

No.	Authors	Title	Date
743	Sundermeyer, J. N., and R. L. Weaver	On crack identification and characterization in a beam by nonlinear vibration analysis	Dec. 1993
744	Li, L., and N. R. Sottos	Predictions of static displacements in 1–3 piezocomposites	Dec. 1993
745	Jones, S. W.	Chaotic advection and dispersion	Jan. 1994
746	Stewart, D. S., and J. Yao	Critical detonation shock curvature and failure dynamics: Developments in the theory of detonation shock dynamics	Feb. 1994
747	Mei, R., and R. J. Adrian	Effect of Reynolds-number-dependent turbulence structure on the dispersion of fluid and particles	Feb. 1994
748	Liu, Z.-C., R. J. Adrian, and T. J. Hanratty	Reynolds-number similarity of orthogonal decomposition of the outer layer of turbulent wall flow	Feb. 1994
749	Barnhart, D. H., R. J. Adrian, and G. C. Papen	Phase-conjugate holographic system for high-resolution particle image velocimetry	Feb. 1994
750	Qi, Q., W. D. O'Brien Jr., and J. G. Harris	The propagation of ultrasonic waves through a bubbly liquid into tissue: A linear analysis	Mar. 1994
751	Mittal, R., and S. Balachandar	Direct numerical simulation of flow past elliptic cylinders	May 1994
752	Anderson, D. N., J. R. Dahlen, M. J. Danyluk, A. M. Dreyer, K. M. Durkin, J. J. Kriegsmann, J. T. McGonigle, and V. Tyagi	Thirty-first student symposium on engineering mechanics, J. W. Phillips, coord.	May 1994
753	Thoroddsen, S. T.	The failure of the Kolmogorov refined similarity hypothesis in fluid turbulence	May 1994
754	Turner, J. A., and R. L. Weaver	Time dependence of multiply scattered diffuse ultrasound in polycrystalline media	June 1994
755	Riahi, D. N.	Finite-amplitude thermal convection with spatially modulated boundary temperatures	June 1994
756	Riahi, D. N.	Renormalization group analysis for stratified turbulence	June 1994
757	Riahi, D. N.	Wave-packet convection in a porous layer with boundary imperfections	June 1994
758	Jog, C. S., and R. B. Haber	Stability of finite element models for distributed-parameter optimization and topology design	July 1994
759	Qi, Q., and G. J. Brereton	Mechanisms of removal of micron-sized particles by high-frequency ultrasonic waves	July 1994
760	Shawki, T. G.	On shear flow localization with traction-controlled boundaries	July 1994
761	Balachandar, S., D. A. Yuen, and D. M. Reuteler	High Rayleigh number convection at infinite Prandtl number with temperature-dependent viscosity	July 1994
762	Phillips, J. W.	Arthur Newell Talbot—Proceedings of a conference to honor TAM's first department head and his family	Aug. 1994
763	Man., C. S., and D. E. Carlson	On the traction problem of dead loading in linear elasticity with initial stress	Aug. 1994
764	Zhang, Y., and R. L. Weaver	Leaky Rayleigh wave scattering from elastic media with random microstructures	Aug. 1994
765	Cortese, T. A., and S. Balachandar	High-performance spectral simulation of turbulent flows in massively parallel machines with distributed memory	Aug. 1994
766	Balachandar, S.	Signature of the transition zone in the tomographic results extracted through the eigenfunctions of the two-point correlation	Sept. 1994
767	Piomelli, U.	Large-eddy simulation of turbulent flows	Sept. 1994
768	Harris, J. G., D. A. Rebinsky, and G. R. Wickham	An integrated model of scattering from an imperfect interface	Sept. 1994

List of Recent TAM Reports (cont'd)

No.	*Authors*	*Title*	*Date*
769	Hsia, K. J., and Z. Xu	The mathematical framework and an approximate solution of surface crack propagation under hydraulic pressure loading	Sept. 1994
770	Balachandar, S.	Two-point correlation and its eigen-decomposition for optimal characterization of mantle convection	Oct. 1994
771	Lufrano, J. M., and P. Sofronis	Numerical analysis of the interaction of solute hydrogen atoms with the stress field of a crack	Oct. 1994
772	Aref, H., and S. W. Jones	Motion of a solid body through ideal fluid	Oct. 1994
773	Stewart, D. S., T. Aslam, J. Yao, and J. B. Bdzil	Level-set techniques applied to unsteady detonation propagation	Oct. 1994
774	Mittal, R., and S. Balachandar	Effect of three-dimensionality on the lift and drag of circular and elliptic cylinders	Oct. 1994
775	Stewart, D. S., T. D. Aslam, and Jin Yao	The evolution of detonation cells	Nov. 1994
776	Aref, H.	On the equilibrium and stability of a row of point vortices	Nov. 1994
777	Cherukuri, H. P., T. G. Shawki, and M. El-Raheb	An accurate finite-difference scheme for elastic wave propagation in a circular disk	Nov. 1994
778	Li, L., and N. R. Sottos	Improving hydrostatic performance of 1–3 piezocomposites	Dec. 1994
779	Phillips, J. W., D. L. de Camara, M. D. Lockwood, and W. C. C. Grebner	Strength of silicone breast implants	Jan. 1995
780	Xin, Y.-B., K. J. Hsia, and D. A. Lange	Quantitative characterization of the fracture surface of silicon single crystals by confocal microscopy	Jan. 1995
781	Yao, J., and D. S. Stewart	On the dynamics of multi-dimensional detonation	Jan. 1995
782	Riahi, D. N., and T. L. Sayre	Effect of rotation on the structure of a convecting mushy layer	Feb. 1995
783	Batchelor, G. K., and TAM faculty and students	A conversation with Professor George K. Batchelor	Feb. 1995
784	Sayre, T. L., and D. N. Riahi	Effect of rotation on flow instabilities during solidification of a binary alloy	Feb. 1995